Cell cycle-associated expression patterns predict gene function in mycobacteria

Running title: Transcriptional compartmentalization of the *Mtb* cell cycle

Aditya C. Bandekar[1], Sishir Subedi[2], Thomas R. Ioerger[2], Christopher M. Sassetti[1]*

[1]Department of Microbiology and Physiological Systems, University of Massachusetts Medical School, Worcester, MA, 01605, USA

[2]Department of Computer Science and Engineering, Texas A&M University, College Station, TX, 77843, USA

*Correspondence: christopher.sassetti@umassmed.edu

Abstract

While the major events in prokaryotic cell cycle progression are likely to be coordinated with transcriptional and metabolic changes, these processes remain poorly characterized. Unlike many rapidly-growing bacteria, DNA replication and cell division are temporally-resolved in mycobacteria, making these slow-growing organisms a potentially useful system to investigate the prokaryotic cell cycle. To determine if cell-cycle dependent gene regulation occurs in mycobacteria, we characterized the temporal changes in the transcriptome of synchronously replicating populations of *Mycobacterium tuberculosis* (*Mtb*). We report that ~16% of genes display a sinusoidal expression pattern with a period consistent with the cell cycle. During cytokinesis, the timing of gene induction could be used to predict the timing of gene function, as mRNA abundance correlated with the order

in which proteins were recruited to the developing septum. Similarly, the expression pattern of primary metabolic genes could be used to predict the relative importance of these pathways for different cell cycle processes. Pyrimidine synthetic genes peaked during DNA replication and their depletion caused a filamentation phenotype that phenocopied defects in this process. In contrast, the IMP dehydrogenase *guaB2* dedicated to guanosine synthesis displayed the opposite expression pattern and its depletion perturbed septation. Together, these data imply obligate coordination between primary metabolism and cell division, and identify periodically regulated genes that can be related to specific cell biological functions.

Introduction

Much of prokaryotic cell biology has been elucidated under rapid-growth conditions in which chromosomal replication takes longer than the doubling time of the cell (Helmstetter and Cooper, 1968), (Cooper and Helmstetter, 1968). Under these conditions, the production of complete chromosomes for daughter cells is ensured via the simultaneous initiation of multiple rounds of DNA replication, and it is not possible for cells to temporally segregate DNA replication from cytokinesis as is seen in the eukaryotic cell cycle. However, this paradigm may not apply to many, if not most, of the bacteria in the environment. For example, *Caulobacter crescentus* exploits a specialized developmental program that produces distinct sessile and motile cells, which is associated with a strict cell cycle that segregates DNA replication from cytokinesis. More generally, most of the bacterial biomass in nutrient poor natural environments is likely to persist in slow-growing states (Gibson et al., 2018). When these conditions are modeled in nutrient-restricted

47 *Escherichia coli*, major cellular events become restricted into distinct cell cycle periods
48 designated, "B", "C", and "D"; in which DNA replication is restricted to the C period. The B
49 and D periods occupy the time before or after C, respectively, and are divided by
50 cytokinesis (Kubitschek and Newman, 1978)(Skarstad et al., 1983). Similarly,
51 mycobacteria are slow-growing organisms, with doubling times that range from 3 hours to
52 several days, which appear to constitutively employ this type of segregated cell cycle.
53 While an ordered cell cycle may be more common in prokaryotes than generally
54 appreciated, it has only been investigated in a limited number of systems.
55
56 The prokaryotic cell cycle has been most thoroughly studied in the aquatic bacterium, *C.*
57 *crescentus*, largely because it is possible to produce bacterial cultures in which cells are
58 replicating synchronously with respect to the cell cycle. As a result, the only genome-wide
59 transcriptional profiles of synchronously-replicating bacteria have been produced in this
60 species. These studies identified periodic fluctuations in mRNA abundance that correlated
61 with the cell cycle (Laub et al., 2000), (Fang et al., 2013) and led to the elucidation of a
62 regulatory cascade that controls cell cycle progression and cellular differentiation that
63 appears to be conserved in other alphaproteobacteria (Brilli et al., 2010). In addition to
64 these regulators of cell cycle progression, 19% of the genome was found to be periodically
65 expressed (Laub et al., 2000). These genes included those involved in primary metabolic
66 processes that are not directly associated with cell cycle progression, suggesting that major
67 cellular events, such as DNA replication and cytokinesis, may be coordinated with other
68 aspects of cellular physiology. These apparent links between metabolism and cell cycle are
69 consistent with a number of studies in model organisms, where metabolites such as

NADH(Zhang et al., 2018) and ATP (Yaginuma et al., 2015) oscillate according to the cell cycle in *E. coli*; and UDP-glucose levels coordinate cell division timing with nutrient availability in both B*. subtilis* (Weart et al., 2007) and *E. coli* (Hill et al., 2013). While these data indicate that cell cycle progression is likely coupled with some aspects of primary metabolism, it remains unclear how these processes interact and whether insights from transcriptional profiling in *C. crescentus* are generalizable are to more diverse bacteria.

We sought to extend these paradigms to mycobacteria, a genus that includes relatively rapid growing environmental organisms, such as *M. smegmatis*, and slower growing pathogenic species such as *M. tuberculosis* (Mtb) and *M. bovis*. The cell cycle has been extensively characterized in both fast- and slow-growing mycobacteria using single-cell analyses of strains engineered to express fluorescent markers of DNA replication and cytokinesis. These studies show that DNA replication occurs only once per cycle in the majority of cells, and re-initiation of replication before division occurs only rarely (Santi et al., 2013) (Santi and McKinney, 2015)(Trojanowski et al., 2015)(Logsdon et al., 2017) (Trojanowski et al., 2017). While the relative durations of the cell cycle phases can be influenced by the environment and stochastic factors such as birth length (Logsdon et al., 2017), the average duration of the B, C, and D periods in Mtb are generally in the range of 6-8 hours, 9-12 hours, and D~6-9 hours, respectively (Logsdon and Aldridge, 2018).

These observations are consistent with studies of synchronously-replicating cultures of *Mtb*, which can be generated using a mutant strain that harbors a cold-sensitive (cos) allele of the DNA replication initiator DnaA (Nair et al., 2009). This *Mtbcos* strain is unable to

initiate a new round of DNA replication at 30ºC. Upon release into the permissive temperature (37ºC), cultures synchronously incorporate 5,6-^{3}H-uracil into alkali stable DNA for 11 hours, consistent with the C period length observed in single cells. The ability to produce synchronously replicating cultures that recapitulate the behavior of single cells makes mycobacteria an attractive system to investigate cell cycle-associated transcriptional changes.

Using the *Mtbcos* strain, we determined the transcriptional profile of synchronously replicating cultures across the cell cycle, and report that 16% of the genome meets strict criteria for periodic gene expression. Only a small fraction of the periodically-regulated gene sets of *Mtb* and *C. crescentus* overlap, suggesting that the links between cell cycle and metabolism are species-specific. We demonstrate that mRNA expression patterns in *Mtb* reflect the time at which the encoded proteins are incorporated into the developing septum, suggesting that functional information can be inferred from the kinetics of gene expression. Using this framework, we discover an unanticipated functional specialization of distinct nucleotide anabolic pathways. These observations show that DNA replication and cytokinesis are coordinated with different primary metabolic pathways, expanding the processes that are associated with these essential cellular events.

Results

DNA replication and cytokinesis are segregated in synchronously growing populations of *Mtb*

We generated synchronously replicating cultures of *Mtb* using the temperature-sensitive *Mtbcos* strain (Nair et al., 2009). Chromosomal replication was uniformly inhibited by incubating this strain at 30ºC for 36 hours. Upon shift to the permissive temperature (37ºC), the optical density ($Absorbance_{600}$) of both the *Mtbcos* mutant and a wild type control culture increased throughout a 54 hour time course, demonstrating that nutrients did not become limiting. While the control culture grew at a constant rate over this period, the *dnaAcos* strain showed a reproducible multiphasic growth pattern, an initial indication that cellular metabolism may be linked to cell cycle events (**Fig1A)**.

In order to estimate the efficiency of the synchronization and to delineate cell cycle periods, we collected cells every three hours and monitored chromosomal replication and cytokinesis. The phosphothreonine-binding protein, FhaA, marks sites of division (Gee et al., 2012), and we used a fluorescent allele of this protein to calculate a "septation index" that corresponded to the fraction of cells with FhaA localization at midcell. While the septation index of a control culture of asynchronous cells (*MtbRv*) was constant throughout the time course, this metric varied in a periodic manner in the *Mtbcos* strain. The majority of cells arrested at the non-permissive temperature had an FhaA focus at midcell, which is likely an artifact of the DnaA inactivation. The septation index of *Mtbcos* cells quickly decreased upon shift to the permissive temperature, falling below the index of unsynchronized cultures by 12 hours. Septation reached a peak in the synchronized cultures between 27 and 33 hours after release, marking the cytokinesis phase of the cell cycle **(Fig1B)**.

To monitor chromosomal replication, we devised a quantitative PCR assay to quantify the relative abundance of DNA at the origin (ori) and terminus (ter) of replication. Upon initiation of replication, the cell will have an ori:ter ratio of 2:1, and this ratio should be maintained until the terminus is duplicated. As we observed for septation index, the ori:ter ratio remained constant in unsynchronized cultures. In contrast, the ori:ter ratio peaked twice in the synchronized cultures **(Fig 1C)**. The first peak lasted for a duration of approximately 12 hours (between 15h-27h post release) and second one lasted between 48-hrs post release and the end of the study. Based on these data, we estimate that our time course captured approximately 1.5 cell cycles. Both the septation index and ori/ter ratio varied by approximately 50% of the range expected of fully synchronized cells, indicating that the synchrony of our cultures was incomplete. Regardless, these observations indicated that DNA replication is temporally segregated from cytokinesis, and the cultures were sufficiently synchronized to perform transcriptional profiling.

Periodic gene expression correlates with cell cycle progression

In order to investigate whether gene expression changes are associated with major cellular events like DNA replication and cytokinesis, we profiled mRNA abundance in synchronized cultures every 3 hours across a 54 hour time course. After normalization and scaling, we first assessed correlation patterns in the dataset. The initial time point after temperature shift to 37ºC (0hr) was uncorrelated with the rest of the datasets, presumably due to an adjustment to the temperature shift and was omitted from subsequent analyses. For the remaining data, we found the highest degree of correlation between adjacent time points,

as expected for a time-resolved dataset **(Fig 2A).** While this was generally true for both the synchronized *Mtbcos* and unsynchronized *MtbRv* strains, the correlation matrix from the *Mtbcos* cultures displayed a distinct three-block structure suggesting the presence of transcriptionally distinct phases. This structure is even more apparent upon hierarchical clustering, which revealed a pattern of gene expression consistent with an ordered progression of events throughout the time course (**FigS1A**).

To take advantage of both replicate measurements and the relatedness of adjacent time points, we used a Gaussian Process (GP) smoothing approach to estimate relative expression levels of each gene across the time course **(Fig S1B)**. The expression of many genes with known cell-cycle related functions were found to peak during the appropriate period. For example, genes that are important for cell division, such as the regulator, *mtrA* (Plocinska et al., 2012) or the septal components, *sepF* (Gola et al., 2015) and *sepIVA* (Wu et al., 2018), peak in expression once during cytokinesis. Similarly, genes important for DNA replication, such as those encoding DNA primase (*dnaG)* and the replicative polymerase (*polA)* display two expression peaks during this time course, corresponding to DNA replication **(Fig2B)**. In addition, we found that the expression pattern of several primary metabolic pathways mirrored these cell-cycle related genes, and suggested alterations in metabolic flux. For example, genes necessary for arginine biosynthesis were co-regulated and had opposing expression patterns to genes involved in arginine catabolism **(Fig2B)**.

We sought to more formally define genes with an expression pattern consistent with cell cycle progression. First, we removed genes with correlated expression patterns in

184 synchronized and unsynchronized cultures to minimize the effect of changes in culture
185 conditions during the time course. Next, we fit the gaussian smoothed values for each gene
186 to a sinusoidal function with the expected period of the *Mtb* cell cycle, optimizing the
187 parameters for trend, amplitude, period and phase. Genes with a period outside the range
188 of reasonable expectations based on the *Mtb* cell cycle were filtered out, along with genes
189 with low overall expression or high variance between replicates. A goodness-of-fit criterion
190 based on curve fitting residuals was applied, which maximized the difference in genes
191 discovered in synchronized versus unsynchronized cultures. These criteria produced a 2.5-
192 fold enrichment in genes discovered in the synchronized data set, and 617 genes were
193 categorized as periodically expressed (**Fig 2C**; **Supplementary Table 2).** This gene set
194 represented all major functional categories (**Fig2D)**.
195
196 Clustering this set of periodically-regulated genes further highlighted the association
197 between gene function and cell cycle stage. Genes were distributed into 18 clusters using
198 hierarchical clustering of the *Mtbcos* expression profiles **(FigS2),** producing groups of
199 coordinately regulated genes with peak expression values ranging across the time course.
200 Eight of these clusters reflected expression profiles that peak during DNA replication
201 **(Fig2E)**. In these clusters, we find 18 genes (parA, mtr, Rv1341, pyrF, dgt, Rv2927c, rnhB,
202 dnaG, ruvB, hpt, pyrH, deaD, mfd, polA, mrp, uvrD1, helY and mesJ) with defined roles in
203 DNA replication, repair or biogenesis, further indicating that expression patterns were
204 consistent with gene function.
205

The periodically regulated gene set (617 genes) in *Mtb* represents 16% of the genome, which is a similar fraction as the 19% of the *C crescentus* genome previously found to be cell cycle associated (Laub et al., 2000)(Fang et al., 2013). In order to investigate whether similar cellular functions are periodically regulated in these phylogenetically diverse organisms, we compared the expression patterns of orthologous genes. Out of the 880 mutual orthologs identified as being reciprocal best BLAST matches, 231 genes were defined as cell cycle regulated in *C. crescentus* by virtue of being differentially expressed over time in synchronized cultures (Fang et al., 2013) and we found 176 to be periodically expressed in *Mtb* with an overlap of 36 genes (**Fig2F, Supplementary Table 3).** This overlap between the two gene sets was greater than what would be expected from random gene sets of the same size ($p<0.03$) and contains a number of genes with known cell cycle associated functions, such as the DNA replication initator, *dnaA*, the ClpXP degradation system that controls cell cycle progression in Caulobacter via CtrA degradation (Jenal and Fuchs, 1998) (Vass et al., 2016), nucleotide metabolism (*dgt, thyA*) and DNA integrity (*uvrD*). However, the modest degree of overlap also suggests that independent sets of genes are periodically expressed in these two phylogenetically distinct organisms.

mRNA abundance predicts the order of assembly of mycobacterial divisome components and regulators

The order in which large multicomponent structures, such as the flagellum, are assembled in bacteria can be predicted based on the transcriptional regulation of the corresponding genes(Kalir et al., 2001). Based on this "just in time" transcription model (Zaslaver et al., 2004), we hypothesized that the assembly of the large complex of proteins necessary for

cell division, aka the "divisome", may follow the same principles and provide a model to test whether mRNA abundance could be used to predict the timing of gene function in our system. To test this model, we assessed the temporal coincidence between mRNA abundance and protein localization at the developing and maturing septum.

To broadly identify genes that are induced during cytokinesis (27-33h), we identified genes that only peak once in the time course **(Supplementary Table 1**) and clustered genes based on similar expression patterns **(Fig3A).** Within the clusters that peak in expression at the appropriate times, we found a number of genes known to be involved in cytokinesis (Fig3A). The first to be induced was *ftsZ*, the tubulin-like nucleator of the septum, and the septally-localized Ser/Thr kinase, *pknD*. This was followed by the expression of genes encoding several divisome-associated proteins, FtsW, SepIVA, and LamA. After these, we found the gene encoding the new pole landmark protein, DivIVA, was induced. To determine if the timing of expression predicted the order of assembly, we chose three genes, *pknD*, *ftsW* and *divIVA* which peaked in expression early, in the middle, and late during the cytokinesis window, respectively. Pairs of these proteins were fused with fluorescent tags and their cellular location was determined by time lapse microscopy in *M smegmatis*, a related mycobacterial species that expresses orthologs of these proteins and is a more experimentally tractable model of mycobacterial division (Kieser and Rubin, 2014). Dual-color fluorescence imaging revealed that PknD, FtsW, and DivIVA appear at the developing septum in the order predicted by mRNA abundance (**Fig 3B-D**). Although not directly addressed in our experiments, it is likely that order of localization at the septum is independent of transcriptional regulation because PknD, and DivIVA fusion

proteins were expressed from constitutive promoters. Instead, the transcriptional order correlates with assembly, which appears to be dictated at the posttranscriptional level.

Guanosine synthesis influences cytokinesis in mycobacteria

Having demonstrated that gene expression can predict the timing of gene function, at least in the case of the developing septum, we investigated whether obligate coordination exists between cellular events, such as DNA replication and cytokinesis, and upstream pathways that produce the precursors for these processes. In particular, we focused on nucleotide metabolism by analyzing the expression patterns of enzymes catalyzing anabolic reactions beginning from the tricarboxylic acid cycle precursor, glutamate to the final nucleos(t)ide products. Pyrimidine biogenesis from the very early stages of the *carAB*-encoded reactions down to the *pyrBCDEF*-encoded reactions were most highly expressed during the C phase (at ~12 hours and ~48 hours), consistent with previous reports of an increased production of thymine nucleotides during DNA replication in *E coli* (Lark, 1961). This also corroborates reports of nucleotide pool sizes in *E coli* being insufficient for chromosome replication and requiring *de novo* synthesis before the onset of the DNA replication phase (Huzyk and Clark, 1971). Unexpectedly, the converse expression pattern was observed for the first reaction unique to guanosine synthesis, peaking at ~21hours. While both adenosine and guanosine purine rings are synthesized from the common precursor inosine monophosphate (IMP), the IMP dehydrogenase GuaB2 catalyses the *first* dedicated reaction unique to GMP synthesis. *guaB2* peaked in expression during cytokinesis (**Fig4A)**. Genes dedicated to synthesizing adenosine from IMP, *purB* and *amk,* did not appear to be cell cycle regulated.

The reciprocal expression patterns of pyrimidine and guanosine synthetic genes suggested that the requirement for these metabolites varied across the cell cycle and these requirements were associated with distinct cellular events. To investigate this hypothesis, we generated mutant *Mtb* strains in which synthesis of pyrimidines or guanosine was inhibited via the inducible genetic depletion of the PyrE or GuaB2 proteins, respectively. Each gene was fused to a C-terminal DAS+4 tag (DAS) that facilitated Clp protease-mediated degradation upon removal of anhydrotetracycline (aTc). In both cases, protein depletion inhibited bacterial growth (**Fig4B**), consistent with the essentiality of these pathways (DeJesus et al., 2017). As *Mtb* expresses three GuaB paralogs, we verified that GuaB2 is essential for guanosine synthesis by supplementing the *guaB2-DAS* strain with 200uM guanine or guanosine. Consistent with previous studies (Singh et al., 2017), guanine partially rescued the growth defect of the depleted strain, whereas guanosine supplementation led to complete rescue (**Fig4C)**.

The inverse expression patterns of *pyr* genes and *guaB2* implied increased *de novo* synthesis of pyrimidine nucleotides and guanosine was required for DNA synthesis or cytokinesis, respectively. To test this hypothesis, we used morphological criteria to infer which cellular process were primarily impacted by the inhibition of these nucleotide synthetic pathways. PyrE depletion resulted in cell elongation before growth arrest. The mean cell length increased from 3.3uM to 4.2uM upon PyrE depletion (**Fig4D**). This phenotype was similar to DNA gyrase GyrB depletion and cells treated with the gyrase inhibiting fluoroquinolone, moxifloxacin **(Fig4D)**, which disrupts DNA replication and

causes cell filamentation in *E coli* (Diver and Wise, 1986). In contrast, GuaB2-depleted cells were the same length as wild type, but many of the growth arrested cells had bulges at midcell or one pole, suggesting that GuaB2 depletion may influence cell division **(Fig4D)**. To determine if these bulges represented misshapen septa leading to aberrant cytokinesis, we performed time-lapse microscopy in *M. smegmatis* cells treated with a specific chemical inhibitor of GuaB2 (VCC234718). Similar to genetic depletion, chemical inhibition of the GuaB2 enzyme also inhibited growth and produced bulges at midcell or one pole **(Fig4E)**. Time-lapse microscopy revealed that cells began to bulge at midcell by the completion of 1-2 cell cycles after the initiation of VCC234718 treatment, and that misshapen poles were derived from these bulges. Taken together, these observations imply that the cellular requirement for guanosine increases during cytokinesis, and that this requirement is reflected in the aberrant septation of guanosine-depleted cells.

FtsZ is among the most abundant proteins in the cell and this tubulin-like protein binds and hydrolyzes GTP (de Boer et al., 1992) as it undergoes the cycles of polymerization and depolymerization necessary for septation (Bisson-Filho et al., 2017). This GTP requirement suggested a possible mechanistic connection between guanosine nucleotide levels and septation. To investigate whether the effect of guanosine depletion on septation could be attributed to altered FtsZ dynamics, we determined the effect of inhibiting both processes simultaneously using the GuaB2 inhibitor VCC234718 and C109, an inhibitor of FtsZ GTPase activity and polymerization (Hogan et al., 2018). Consistent with the hypothesized mechanistic link, we observed significant antagonism between these compounds. Even at concentrations of VCC234718 that alone had no effect on growth (0.5 - 4uM), this

compound consistently increased the IC50 of C109 (**Fig4F)**. In contrast, we found no interaction between VCC234718 and spectinomycin, an inhibitor of another major GTP consuming pathway, translation. C109, has previously been found to act additively with PCI90723, a compound that stabilizes the FtsZ filament. The opposite antagonistic interaction we observed between C109 and a GuaB2 inhibitor implies that guanosine inhibition inhibits polymerization, an effect that is consistent with the known GTP requirement for FtsZ polymerization.(de Boer et al., 1992), (Mukherjee and Lutkenhaus, 1998). Taken together, these data are consistent with a model in which transcriptional induction of GuaB2 during cytokinesis coincides with the increased consumption of GTP by FtsZ, and the septal defects observed on guanosine depletion are related to defects in FtsZ dynamics.

Discussion

Previously, transcriptomic studies of the prokaryotic cell cycle have been limited to the *C. crescentus* model, due to the inability to generate robust synchronously replicating populations in other organisms. In this study, we leveraged a genetic strategy to synchronize *Mtb* cultures, and characterized cell cycle associated transcriptional changes in this organism. Comparisons between our *Mtb* studies and previously generated *C. cresentus* data are limited by a number of technical differences, including the method and degree of synchronization, that likely limited our ability to discern periodic patterns of relatively small amplitude in the *Mtb* dataset. Regardless, our findings are broadly comparable to observations in *C. crescentus*, as we found that a similar fraction of the genome is differentially expressed across the cell cycle in both systems, and a small but

significant fraction of orthologous genes are periodically-regulated in both. Despite these similarities, the majority of cell-cycle associated transcriptional changes (71% of *C. crescentus* genes and 80% of *Mtb* genes) were unique to each organism. Thus, despite some similarities, our analysis indicates that cell cycle progression is associated with distinct transcriptional networks in these structurally and phylogenetically divergent organisms.

In a number of cases, we found that increases in mRNA abundance could be used to associate genes with temporally-resolved cell cycle events, such as septation. The sequential expression of divisome components as cell division progresses has been observed previously in *C. crescentus* (Laub et al., 2000). We provide functional evidence that this hierarchical expression pattern is associated with the order of divisome assembly in mycobacteria by demonstrating that the timing of gene induction correlates with the recruitment of the encoded proteins to the developing septum. Based on transcriptional data, we inferred the following order of assembly at the mycobacterial septum: FtsZ>PknD>FtsW>LamA>SepIVA>DivIVA. The recruitment of these proteins spans sequential processes of divisome assembly and new pole biogenesis. FtsZ initially marks the future division site (Bi and Lutkenhaus, 1991), facilitating the recruitment of divisome components such as FtsW (Wang et al., 1998) and SepIVA (Wu et al., 2018). The arrival of LamA at the later stages of assembly is consistent with its role in delaying septation and thereby promoting asymmetric cell division(Rego et al., 2017). DivIVA is thought to be recruited to the negative curvature of the new pole after septation(Lenarcic et al., 2009)(Ramamurthi and Losick, 2009)(Meniche et al., 2014) and the segregation of

daughter cell cytoplasm (Santi et al., 2013). While these observations highlight that gene expression pattern can be used to predict the order of complex assembly, the outcome of this coordination remains unclear. As only a subset of currently known septal components were found to be periodically expressed, transcriptional regulation is unlikely to be the primary determinant of assembly order. Instead, this type of hierarchical gene expression has also been proposed as a mechanism to maximize efficiency by restricting protein expression to the period when it is needed (Kalir et al., 2001)(Zaslaver et al., 2004). Regulation of divisome assembly and function likely involves additional posttranslational mechanisms, as we found that the Ser/Thr kinase, PknD, is recruited relatively early in septal development and previous work described an important role for the Ser/Thr phosphatase, PstP, in cell division(Sharma et al., 2016), (Iswahyudi et al., 2019). While it remains possible that transcriptional regulation controls some aspects of septation, our data only show that expression pattern can predict the timing of gene function.

The observed periodic expression of primary metabolic functions suggested the importance of coordinating cell cycle events with the upstream pathways that provide their precursors. This model is supported by our finding that pyrimidine synthetic genes peak during a distinct cell cycle period than the dedicated guanosine synthetic gene, GuaB2; and that the depletion of these genes primarily disrupts different cellular processes.
It is not surprising that the requirement for pyrimidines would increase during DNA synthesis, as *de novo* nucleotide synthesis is necessary to replicate the chromosome(Huzyk and Clark, 1971). However, the distinct cytokinesis defect observed upon GuaB2 depletion was unanticipated. Guanine nucleotides are important for a myriad of cellular processes,

including DNA replication, transcription, translation, and the biosynthesis of cofactors and polysaccharides. We speculate that the septation defect we observe upon GuaB2 depletion is related to the relatively low affinity of FtsZ for GTP. An accurate determination of nucleotide pool sizes in mycobacteria is still an open question (Warner et al., 2013), but in *E coli,* FtsZ has ~500-fold lower affinity for GTP than the DnaE1 replicative DNA polymerase (K_m $FtsZ_{GTP}$ =1mM(Arjes et al., 2015) ; $K_m DnaE1_{GTP}$=2uM(Rock et al., 2015)). Futhermore, the reported intracellular concentration of GTP(Buckstein et al., 2008) would support only one-half of the V_{max} of FtsZ (Arjes et al., 2015). These data indicate that GTP levels may limit FtsZ dynamics. It is likely that GuaB2 depletion leads to aberrant FtsZ activity and not a loss of function, since genetic depletion of FtsZ leads to filamentation (Ehrt et al., 2005), a phenotype distinct from the one we observe upon GuaB2 depletion. Instead, alterations in FtsZ filament length or rate of turnover are likely to underly these defects.

Both DNA replication and cell division are essential processes that have been the focus of antibacterial drug discovery efforts(Warner et al., 2013)(Sass and Brötz-Oesterhelt, 2013). In most cases, these efforts focus on inhibiting a limited number of physical components of the bacterial replisome or divisome. Our transcriptional data identified a wide variety of genes that are coordinately expressed with the genes encoding these complexes, and therefore may be required for their activity. While we have only investigated these functional dependencies in the context of nucleotide synthesis, our data suggest that many similar dependencies exist and can be predicted from transcriptional profiles. If so, these

412 data could be used to identify a wealth of new strategies for inhibiting these specific
413 essential cellular processes.
414
415 **Figure Legends**
416 **Figure 1: DNA replication and cytokinesis are segregated in synchronously growing**
417 **populations of Mtb**
418 (A) Growth of *Mtbcos* (left) and *MtbRv* (right) after release into permissive temperature
419 37ºC. X axis: hours at 37ºC. Y axis: $Absorbance_{600}$
420 (B) FhaA septation index assay to determine cytokinesis phase. Percentage of *Mtbcos* (left)
421 and *MtbRv* (right) populations containing an FhaA-venus focus localized at midcell after
422 release into permissive temperature. Data points are representative of two biological
423 replicates. Blue line is smoothed via the Gaussian process. The blue band indicates 95%
424 confidence interval. Significant difference between *Mtbcos* and *MtbRv* curves was
425 determined using a likelihood ratio test which determines if the data is fit best by a
426 combined model (null hypothesis) or separate strain specific models (alternate
427 hypothesis). log_likelihood difference between combined and separate models = -38.489,
428 p-value (chi-squared distribution; df=3) = 1.1e-16.
429 (C) Origin/terminus assay to determine the DNA replication phase. Relative ori/ter ratio of
430 *Mtbcos* (left) and *MtbRv* (right) populations after release in permissive temperature. Data
431 points are representative of two biological replicates. Blue line is smoothed via the
432 Gaussian Process. The blue band indicates 95% confidence interval. Significant difference
433 between *Mtbcos* and *MtbRv* curves was determined using a likelihood ratio test

(log_likelihood difference between combined and separate models = -12.412, p-value (chi-squared distribution; df=3) = 1.679e-05.

Figure 2: Periodic gene expression correlates with cell cycle progression

(A) Correlation matrix of DESeq normalized counts for single replicates of *Mtbcos* (left) and *MtbRv* (right) for all 16 timepoints. (Blue: Pearson's correlation coefficient=0; Yellow: Pearson's correlation coefficient=1).

(B) Normalised DeSeq values of genes involved in DNA replication & cell division (top panel); arginine catabolism & anabolism (bottom panel).

(C) Hierarchical clustering of 617 periodically expressed genes in *Mtbcos* (Similarity metric: centered correlation, Clustering method: centroid linkage).

(D)Fraction of periodically expressed genes present in different Gene Ontology categories.

(E) Clusters containing periodic genes with expression patterns consistent with a role in DNA replication. Known DNA replication genes are listed in each cluster. X axis: hours post release into permissive temperature. Y axis: Normalised DESeq values

(F) Overlap between periodically expressed (*Mtbcos*) and differentially expressed (*C. crescentus*) mutual orthologs. Statistical significance of the overlap was determined using a hypergeometric test. $p<0.03$ for randomly drawing 36 genes in both organisms from the parent set of 880 genes.

Figure 3: mRNA abundance predicts the order of assembly of mycobacterial divisome components and regulators

(A) (Left) Clusters of *Mtbcos* genes with expression patterns that peak during the cytokinesis period. (Right) Scaled relative expression of known cytokinesis genes from these clusters.

(B) (Left) Scaled relative expression of PknD and DivIVA. (Right) Time-lapse imaging of *M smegmatis* expressing PknD-Venus (green) and DivIVA-RFP (red). Time (minutes) before the arrival of DivIVA at midcell is indicated.

(C) (Left) Scaled relative expression of FtsW and DivIVA. (Right) Time-lapse imaging of *M smegmatis* expressing FtsW-Venus (green) and DivIVA-RFP (red). Time (minutes) before the arrival of DivIVA at midcell is indicated.

(D) Time (minutes) between initial arrival of PknD (n=10), FtsW (n=7) and DivIVA at midcell. Error bars indicate mean ± SD. Statistically significant difference between pknD and ftsW determined using an unpaired T-test (α =0.05; p=0.0023). Statistically significant difference between ftsW and divIVA determined using a chi-squared test (α =0.05 ; χ^2=7; df=1; p<0.01).

Figure 4: Guanosine synthesis influences cytokinesis in mycobacteria

(A) Relative expression of IMP dehydrogenase *guaB2* compared to pyrimidine biosynthesis genes *carA*, *carB*, *pyrB*, *pyrC, pyrD, pyrF*

(B) Cumulative growth (Absorbance$_{600}$) of *M tuberculosis guaB-2*DAS (top), *gyrB*-DAS (center), *pyrE*-DAS (bottom) without depletion (solid line) and with depletion (dotted line). Arrows indicate the time during the pre-depletion period when cultures were back diluted into fresh growth medium. Data are represented as mean ± SD of two biological replicates

(C) Growth (Absorbance$_{600}$) of *M tuberculosis guaB2*-DAS ±depletion in the presence of either 200μM guanine or guanosine. Data are represented as mean ± SD of two biological replicates.

(D) *M tuberculosis* cellular phenotypes upon genetic depletion of GuaB2, PyrE, GyrB. Images were obtained after the cessation of growth in depleted cells. In the case of GuaB2, septal bulges (arrowheads) and polar bulges (arrows) are indicated. Histograms indicate the cell length distribution of cells in which the target was either not depleted (gray) or depleted (black). *Mtb* was treated with 0.2μM moxifloxacin for 24 hours and imaged. Histograms indicate the cell length distribution of cells in untreated (gray) or treated cells (black). MFD = Maximum Feret Diameter (1μM ~ 0.11MFD). Statistically significant/non-significant difference between the cell length distributions was determined using the Mann-Whitney test. (p_{guaB2}=0.214; p_{pyrE}<0.001; p_{gyrB}<0.001; $p_{moxifloxacin}$<0.001)

(E) Time-lapse imaging at 20 minute intervals of GFP-expressing *M smegmatis* treated with 2μM VCC234718.

(F) Left: Susceptibility of *M smegmatis* to VCC234718. Data are represented as mean ± SD
Center: Cross titration assay on GFP-expressing *M smegmatis* with the indicated concentrations of VCC234718 and C109. Statistically significant difference between the VCC alone curve and other curves was determined using an extra-sum-of-squares F-test (α=0.05). $p_{(VCC\ 0.5_{\mu}m)}$= 0.0215; $p_{(VCC\ 1_{\mu}M)}$= 0.0284 ; $p_{(VCC2_{\mu}M)}$= 0.0001 ; $p_{(VCC4_{\mu}M)}$= 0.0019
Right: Cross titration assay on GFP-expressing *M smegmatis* with the indicated concentrations of VCC234718 and spectinomycin. The differences between the VCC alone curve and other curves were not significant, as determined using an extra-sum-of-squares

F-test (α =0.05). $p_{(VCC0.5_{\mu}M)}$= 0.9989 ; $p_{(VCC1_{\mu}M)}$= 0.9999 ; $p_{(VCC2_{\mu}M)}$=ambiguous ; $p_{(VCC4_{\mu}M)}$= 0.9978

Supplemental figure legends

FigS1A: Hierarchical clustering of significantly expressed genes in *Mtbcos* (log transformed DESeq normalized counts, centered around the mean, similarity metric: centered correlation, clustering method: centroid linkage). X axis: hours at 37ºC.

FigS1B: Expression profile of the DNA polymerase *polA*. Data from two replicates (yellow and blue dashed lines) , GP fit (solid blue line) and sinusoidal fit (pink dotted line) are shown. Y axis: Normalised DESeq values. The DESeq value for each time point was normalized to the mean polA expression value across all time points.

FigS2: Eighteen Clusters containing the 617 periodic genes in *Mtbcos* (Distance matrix: Euclidean, Clustering method: Hierarchical). Heatmaps represent the expression patterns of the same genes in synchronized (*Mtbcos*) and unsynchronized *(MtbRv)* cultures.

Supplemental tables

Table 1: Normalised DESeq2 values for all detected 2948 genes which were deemed to be significantly expressed. Each value represents the DESeq2 value normalized to the mean value of that gene across time. Genes determined to have one or two peaks in expression are indicated along with their peak cluster assignment.

Table 2: Normalised DESeq2 values for the 617 periodic genes. Each value represents the DESeq2 value normalized to the mean value of that gene across all time points. Periodic gene cluster ID is indicated.

Table3: List of overlapping periodically expressed *Mtb* (this study) and differentially expressed *C crescentus* (Fang et al., 2013) orthologs.

Materials and Methods

Strains

The *Mtbcos* strain was obtained from (Nair et al., 2009). *MtbRv* is the H37Rv strain used as an unsynchronized control. Mtbcos and MtbRv expressing FhaA m-venus were transformed with pKP887 (mycobacterial replicating plasmid MEH expressing MSMEG FhaA-Venus expressed from the MSMEG *fhaA* native promoter (from K.P. Sundaram). *M smegmatis* expressing ftsW-mVenus and divIVA-RFP was transformed with ptb21-ftsW-mVenus-MEK and tb21-divIVA-RFP-MCtH. *M smegmatis* expressing pknD-mVenus and DivIVA-RFP was transformed with p16-pknD-mVenus-MEK (Baer et al., 2014) and tb21-DivIVA-RFP-MCtH. *Mtb* hypomorphs used in this study were generated as part of an earlier study (Johnson et al., 2019) using a controlled protein degradation system described previously(Kim et al., 2011). Three strains were used in this study: *Mtb guaB2*-DAS-Hyg^R+Giles-TetON1-sspB-str^R ; *Mtb* gyrB-DAS-Hyg^R+Giles-TetON6-sspB-str^R *; Mtb* pyrE-DAS-Hyg^R+Giles-TetON1-sspB-str^R. *M smegmatis* expressing green fluorescence contains the plasmid CT161 (m-Venus pMV261 Hyg^R) obtained from the Eric Rubin Lab.

Mtbcos synchronization

Cultures of Mtb*dnaAcos115* generated in a previous study (Nair et al., 2009), MtbH37Rv, Mtb*dnaAcos115*-FhaA-Venus and MtbH37Rv-fhaA-Venus were grown in standard culture media at 37ºC under shaking conditions till OD_{600} 0.4. The cells were shifted to 30ºC for 36

hours. The cultures were then shifted to 37ºC and the cultures were processed for either DNA isolation, RNA isolation or fluorescent microscopy at the following times: 0h, 3h, 6.5h, 9h, 12h, 18.5h, 21h, 27h, 31h, 33h, 36h, 39.5h, 42h, 45.5h, 52h and 55h.

Chromosomal DNA isolation

Chromosomal DNA was isolated from the cell pellet of 5ml culture from each timepoint. Briefly, 0.5 ml of chloroform:methanol (2:1) was added and the mixture was vortexed 5X 1min. 0.5ml of phenol:chloroform was added and the mixture was vortexed for 30 seconds. Finally, 0.5ml of TE buffer was added. This was centrifuged at 12,000g at4C for 5 minutes. The upper phase was mixed with 1 volume of chloroform and vortexed. After centrifugation, the upper phase was added to a new tube and 1/10 volume of 3M sodium acetate and 1 volume of isopropanol was added. Precipitated DNA was spun out of solution and resuspended in 20ul of TE buffer.

Origin:terminus assay

Multiple primer sets (designed using the Primer3 design tool) amplifying 150bp at each location (Origin-0MB region surrounding Rv0001; Terminus –2.2MB region surrounding Rv1949c) of the *Mtb*H37Rv genome were tested for amplification efficiency. Efficiency was calculated from the negative slope of the standard curve of C_T v/s template concentration. The primer sets with the highest and most similar efficiencies for both loci were selected (95% for the origin and 93% for the terminus). Quantitative PCR was done using SYBR green (Biorad iQ SYBR Green Supermix) with 2ng of gDNA template per reaction. Delta Ct values were calculated as $dCt= Ct_{ori}-Ct_{ter}$. 2^-dCt values were then calculated for each

570 timepoint. These values were then divided by the mean 2^-dCt across all timepoints to
571 generate a relative ori/ter ratio for each timepoint.
572
573
574 **Microscopy**
575 Static imaging
576 At each time point post release into 37ºC (Fig1B) or timepoint post genetic depletion of
577 GyrB, GuaB2 and PyrE (Fig4D), 1ml of *Mtb* culture was centrifuged and cells were re-
578 suspended in a phosphate buffered saline solution containing 0.05% Tween80 and 4%
579 paraformaldehyde. These fixed cells were then placed onto an agarose pad and DIC (Fig4D)
580 or wide field fluorescence imaging (Fig1B) was performed with a DeltaVision Personal DV
581 microscope (GE Healthcare) using a 60X oil immersion objective (AP). Cell lengths in Fig4D
582 were determined using CellProfiler™ (Carpenter et al., 2006) which calculates a MFD
583 (Maximum Feret Diameter) which is a measurement of the largest number of pixels
584 between the two ends of the cell obtained while rotating a caliper along all possible angles.
585 The approximate conversion factor of MFD to microns is 0.11. Calculating an MFD is
586 especially useful for measuring mycobacteria since all cells are not strict rods (cells
587 undergo V-snapping prior to resolution of cytokinesis and daughter cell separation). The
588 cell debris observed during GyrB depletion in Fig4D was excluded from cell length
589 quantification by training CellProfiler using CP Analyst™.
590 Live cell imaging
591 10ul of cells in logarithmic phase (OD_{600} 0.2-0.5) were spotted on a glass bottom 24-well
592 plate (MatTek Corporation). 500ul of molten Luria Bertani medium (40-50C) was spread

over the cells and allowed to solidify. For experiments with VCC234718, molten LB containing 2uM final concentration of VCC234718 was prepared before layering over the cells. Time-resolved imaging was performed with a DeltaVision Personal DV wide field fluorescence microscope equipped with Ultimate Focus™ capabilities and an environmental chamber warmed to 37 °C (Applied Precision). Images were taken at 5 or 10 minute intervals.

RNA isolation, library preparation and sequencing

At each timepoint, 45ml culture was pelleted and resuspended in 1ml of TRIzol (Invitrogen) and transferred to lysing matrix tubes (MP Biomedicals: Lysing Matrix B). Cells were lysed in a MP Biomedicals Fast Prep-24 homogenizer (maximum power-6.5, 4 X 30s cycles, rest on ice for 5 minutes in between cycles). RNA was purified according to the manufacturer's directions. RNA cleanup was performed with Qiagen RNeasy Mini kit (74104) omitting the DNase step. Instead, after elution, in-tube DNase treatment was performed using Ambion DNase Turbo. RNeasy cleanup was repeated again with double volumes of RLT and ethanol. RNA was subjected to rRNA removal with Ribozero Bacteria kit (Illumina-MRZB12424). Deep sequencing library was prepared using KAPA Stranded RNASeq kit (KK8401). The RNAseq libraries were sequenced on an Illumina 2500 instrument in paired-end mode, using a read-length of 150+150bp. The mean number of reads per sample was 8.9M (range 4.2-16.5M). The reads were mapped to the H37Rv genome using Burroughs Wheeler Alignment (Li and Durbin, 2009) with default parameter settings. Reads mapping to each ORF were totaled (sense strand only). Because certain loci were over-represented (e.g. rrs, rnpB, ssr, Rv3661, which had counts ~0.5-1M), counts

were truncated to a maximum coverage of 10,000 (reads/nt).

Data normalization, filtering and centering

The global expression profiles of *Mtbcos* samples showed a gradual increase in expression of a few genes that dominate expression at latter time-points. Consequently, a compensatory decrease was observed in expression of other genes, making normalization by traditional reads per kilobase per million (RPKM) mis-representative. To correct for the bias induced by these outliers, the normalization method implemented in DESeq2 (Love et al., 2014) was used, which first normalizes counts by the geometric mean for each gene across samples, and then scales each dataset to have a common median (which is less sensitive to outliers). This was applied to all 64 datasets (2 strains X 2 replicates X 16 time-points) in parallel. As a result, the expression patterns were well-calibrated between time-points, with the medians matched.

To identify a subset of genes with meaningful expression, the average expression over all time-points was calculated for each gene and divided by gene length (in nucleotides). 1070 genes out of 4018 with coverage<0.25 were dropped because expression patterns for genes with low expression are inherently noisy, leaving 2948 genes with coverage>0.25. (Supplementary Table 1). Additionally, we removed 127 genes out of 2948 genes whose expression was >90% correlated between *Mtbcos* and *MtbRv* from subsequent analysis, as their expression patterns were assumed to be determined more by time than by difference in the strains. To center the expression values, the counts were divided by the mean for that gene across all the time points. This was done independently for *Mtbcos* and *MtbRv.*

Gaussian Process Smoothing

In order to meaningfully integrate the data from the two replicates and to smooth out profiles over time, we used a Gaussian Process (GP) to fit the raw data (septation index and ori/ter – Fig1, gene expression- Fig2, Fig3, Fig4).

A GP model is a Bayesian model that estimates the probability distribution over functions using Gaussian distributions for likelihood functions. The advantage of a GP is that it is unbiased and therefore does not require assumptions of form of function. Instead, it only assumes that adjacent time points are better coupled than distant time points and that this correlation is based on Gaussian distributions.

A Gaussian Process is specified by a mean function and a covariance function

$$f(x) \sim GP\big(m(x), k(x, x')\big)$$

A prior mean m(x)=0 and a covariance function, squared exponential is given as:

$$k(x, x') = \sigma^2 \exp\left(-\frac{1}{2}\sum_{i=1}^{d}\frac{(x_i - x'_i)}{l_i^2}\right)$$

where l^2= lengthscale, σ^2 = variance, d = input dimension

We normalized the expression value e(g,t) (with addition of pseudocounts of 10) of each gene g at each time point t by dividing the mean across all time points, and then taking log base *e* transformation so that the normalized value *e'(g,t)* fluctuates with a mean of 0. The formula is given as:

$$e'(g,t) = \log_e e\frac{e(g,t)}{\sum_t^T e(g,t)}$$

Gaussian estimation of the expression levels for a gene at different time points, subject to noise is given as:

$$y = f(x) + \varepsilon \quad \text{where: } \varepsilon \sim N\ (\mu, \sigma_n^2)$$

The predictive distribution for 15 test time points (~ 3 hour intervals, 3-55 hours), $\{x_1, x_2, \ldots., x_*\}$ is specified as:

$$p(f_*|x_*, x, y) = N(m(x_*), k(x_*))$$

where:

$$m(x_*) = k(x_*, x)^T (k(x, x) + \sigma^2 I)^{-1} y$$

$$k(x_*) = k\ (x_*, x_*) - k(x_*, x)^T (k(x, x) + \ \sigma^2 I)^{-1}\ k\ (x_*, x) + \sigma^2$$

We utilized the GPy Python package to fit the relative expression data (value for cos1 and cos2 simultaneously normalized by the mean expression level across all 60 time points for each gene using the following hyperparameters: variance = 1.0, noise variance = 0.1 and lengthscale (range 1 ~ 50) optimized to Maximum Likelihood Estimate (MLE) using a grid search method. After fitting the model, the predicted value (i.e. posterior mean) for each time point can be extracted. **Fig S1B** shows the GP regression obtained for *polA* (Rv 1629: DNA polymerase). Not only do the fitted values from the GP model generally interpolate between the observed data at each time point, they also present a smoother profile by averaging between adjacent time points to reduce noise. The error bands show the uncertainty in the model (95% confidence interval which can be denoted as $\pm 1.96 * \Sigma$. Where Σ is the estimated standard deviation at the X-coordinate from the model based on variance of the training data and surrounding points).

Sinusoidal curve fitting

The function implemented is written as:

$$y = A \sin(\omega t + \Phi) + B + Ct$$

where:

A = Amplitude; ω= Frequency; B= Mean offset; Φ= phase shift; Ct= a linear term to capture a net increasing or decreasing trend in the expression

This function was implemented in the curve_fit() function in Sci Py using non-linear least-squares as described in the Levenberg-Marquardt algorithm. 2758 genes fit the curve to varying degrees. We then used a threshold on the residual of the sinusoidal fit to select significantly periodic genes. This threshold was chosen to maximise the tradeoff of periodic genes in *Mtbcos* versus *MtbRv.* Below are the thresholds implemented and the number of positive attrition genes that passed each cutoff, applied sequentially:

Residual (<0.1) : 918 genes

Amplitude (>0.15) : 753 genes

Slope (<0.1) : 631 genes

Period in range of 10-30 hours : 617 genes (Supplementary Table 2)

Clustering

Genes were clustered based on their expression profiles using hierarchical clustering (*hclust* in R), using the ward.D2 method (Jr, 1963) based on the Euclidean distance between the vectors of normalized expression values averaged between replicates over the 15 time points. The dendogram was then divided into disjoint clusters using *cuttree*.

Peak Assignment

Using the GP fit data, we applied the following criteria to assign a peak to a gene's expression profile. The time series *T* with *n* observations for each gene with smoothed

expression values $\{x_1, x_2, \ldots, x_n\}$ at different time points $\{t_1, t_2, \ldots, t_n\}$ was defined as:

$$T = \{(t_1, x_1), (t_2, x_2), \ldots (t_n, x_n)\}$$

First, to screen out the increasing or decreasing trend at the beginning and end of the time series, and to focus on the cytokinesis phase in the middle of the time course, we excluded the first and last two time points from the peak assignment. Second, to identify well-spaced major peaks across time points, we defined a point x_i as a peak if it has a greater magnitude than its two nearest neighbors on both sides. This is defined as:

$$x_i > x_{i+1}, x_{i+2}, x_{i-1}, x_{i-2} \qquad \forall_i = 3,4, \ldots, n-2$$

Furthermore, to filter out the genes with lower fluctuations, the difference between the magnitude of the highest peak x_h and the global minimum g_{min} was restricted to be greater than 0.5. Additionally, in the case of more than one peak in the time series, all the peaks were constrained to have at least a half magnitude of the highest peak in the expression profile. Finally, a set of peaks *P* for a time series was identified as:

$$P = \{(t_i, x_i) | (x_i > x_{i+1}, x_{i+2}, x_{i-1}, x_{i-2}) \wedge (x_i - g_{min} > 0.5) \wedge (x_i \geq 0.5 * x_h)\} \ \forall_i = 3,4, \ldots, n-2$$

Among the significantly expressed genes, the peak assignment identified 1620 genes with a single peak and 71 genes with two peaks in the *Mtbcos* strain compared to 903 genes with a single peak and 8 genes with two peaks in *MtbRv*. Similarly, 1222 genes in the cos strain and 2344 genes in the wild type did not have any major peak. This once again confirmed that the gene expression levels in the *Mtbcos* strain show significantly higher fluctuations than *MtbRv*.

References

719 Arjes, H.A., Lai, B., Emelue, E., Steinbach, A., and Levin, P.A. (2015). Mutations in the bacterial
720 cell division protein FtsZ highlight the role of GTP binding and longitudinal subunit interactions
721 in assembly and function. BMC Microbiol *15*, 209.

722 Baer, C.E., Iavarone, A.T., Alber, T., and Sassetti, C.M. (2014). Biochemical and Spatial
723 Coincidence in the Provisional Ser/Thr Protein Kinase Interaction Network of Mycobacterium
724 tuberculosis. J. Biol. Chem. jbc.M114.559054.

725 Bi, E., and Lutkenhaus, J. (1991). FtsZ ring structure associated with division in Escherichia coli.
726 Nature *354*, 161–164.

727 Bisson-Filho, A.W., Hsu, Y.-P., Squyres, G.R., Kuru, E., Wu, F., Jukes, C., Sun, Y., Dekker, C.,
728 Holden, S., VanNieuwenhze, M.S., et al. (2017). Treadmilling by FtsZ filaments drives
729 peptidoglycan synthesis and bacterial cell division. Science *355*, 739–743.

730 de Boer, P., Crossley, R., and Rothfield, L. (1992). The essential bacterial cell-division protein
731 FtsZ is a GTPase. Nature *359*, 254–256.

732 Brilli, M., Fondi, M., Fani, R., Mengoni, A., Ferri, L., Bazzicalupo, M., and Biondi, E.G. (2010). The
733 diversity and evolution of cell cycle regulation in alpha-proteobacteria: a comparative genomic
734 analysis. BMC Systems Biology *4*, 52.

735 Buckstein, M.H., He, J., and Rubin, H. (2008). Characterization of Nucleotide Pools as a Function
736 of Physiological State in Escherichia coli. Journal of Bacteriology *190*, 718–726.

737 Carpenter, A.E., Jones, T.R., Lamprecht, M.R., Clarke, C., Kang, I.H., Friman, O., Guertin, D.A.,
738 Chang, J.H., Lindquist, R.A., Moffat, J., et al. (2006). CellProfiler: image analysis software for
739 identifying and quantifying cell phenotypes. Genome Biology *7*, R100.

740 Cooper, S., and Helmstetter, C.E. (1968). Chromosome replication and the division cycle of
741 Escherichia coli Br. Journal of Molecular Biology *31*, 519–540.

742 DeJesus, M.A., Gerrick, E.R., Xu, W., Park, S.W., Long, J.E., Boutte, C.C., Rubin, E.J.,
743 Schnappinger, D., Ehrt, S., Fortune, S.M., et al. (2017). Comprehensive Essentiality Analysis of
744 the Mycobacterium tuberculosis Genome via Saturating Transposon Mutagenesis. MBio *8*.

745 Diver, J.M., and Wise, R. (1986). Morphological and biochemical changes in Escherichia coli
746 after exposure to ciprofloxacin. J Antimicrob Chemother *18*, 31–41.

747 Ehrt, S., Guo, X.V., Hickey, C.M., Ryou, M., Monteleone, M., Riley, L.W., and Schnappinger, D.
748 (2005). Controlling gene expression in mycobacteria with anhydrotetracycline and Tet
749 repressor. Nucleic Acids Res *33*, e21.

750 Fang, G., Passalacqua, K.D., Hocking, J., Llopis, P., Gerstein, M., Bergman, N.H., and Jacobs-
751 Wagner, C. (2013). Transcriptomic and phylogenetic analysis of a bacterial cell cycle reveals
752 strong associations between gene co-expression and evolution. BMC Genomics *14*, 450.

753 Gee, C.L., Papavinasasundaram, K.G., Blair, S.R., Baer, C.E., Falick, A.M., King, D.S., Griffin, J.E.,
754 Venghatakrishnan, H., Zukauskas, A., Wei, J.-R., et al. (2012). A Phosphorylated Pseudokinase
755 Complex Controls Cell Wall Synthesis in Mycobacteria. Sci. Signal. *5*, ra7–ra7.

756 Gibson, B., Wilson, D.J., Feil, E., and Eyre-Walker, A. (2018). The distribution of bacterial
757 doubling times in the wild. Proc Biol Sci *285*.

758 Gola, S., Munder, T., Casonato, S., Manganelli, R., and Vicente, M. (2015). The essential role of
759 SepF in mycobacterial division. Molecular Microbiology *97*, 560–576.

760 Helmstetter, C.E., and Cooper, S. (1968). DNA synthesis during the division cycle of rapidly
761 growing Escherichia coli Br. Journal of Molecular Biology *31*, 507–518.

762 Hill, N.S., Buske, P.J., Shi, Y., and Levin, P.A. (2013). A Moonlighting Enzyme Links Escherichia
763 coli Cell Size with Central Metabolism. PLoS Genet *9*, e1003663.

764 Hogan, A.M., Scoffone, V.C., Makarov, V., Gislason, A.S., Tesfu, H., Stietz, M.S., Brassinga, A.K.C.,
765 Domaratzki, M., Li, X., Azzalin, A., et al. (2018). Competitive Fitness of Essential Gene
766 Knockdowns Reveals a Broad-Spectrum Antibacterial Inhibitor of the Cell Division Protein FtsZ.
767 Antimicrob Agents Chemother *62*, e01231-18, /aac/62/12/e01231-18.atom.

768 Huzyk, L., and Clark, D.J. (1971). Nucleoside Triphosphate Pools in Synchronous Cultures of
769 Escherichia coli. Journal of Bacteriology *108*, 74–81.

770 Iswahyudi, Mukamolova, G.V., Straatman-Iwanowska, A.A., Allcock, N., Ajuh, P., Turapov, O.,
771 and O'Hare, H.M. (2019). Mycobacterial phosphatase PstP regulates global serine threonine
772 phosphorylation and cell division. Sci Rep *9*, 8337.

773 Jenal, U., and Fuchs, T. (1998). An essential protease involved in bacterial cell-cycle control. The
774 EMBO Journal *17*, 5658–5669.

775 Johnson, E.O., LaVerriere, E., Office, E., Stanley, M., Meyer, E., Kawate, T., Gomez, J.E., Audette,
776 R.E., Bandyopadhyay, N., Betancourt, N., et al. (2019). Large-scale chemical–genetics yields new
777 M. tuberculosis inhibitor classes. Nature *571*, 72–78.

778 Jr, J.H.W. (1963). Hierarchical Grouping to Optimize an Objective Function. Journal of the
779 American Statistical Association *58*, 236–244.

780 Kalir, S., McClure, J., Pabbaraju, K., Southward, C., Ronen, M., Leibler, S., Surette, M.G., and
781 Alon, U. (2001). Ordering Genes in a Flagella Pathway by Analysis of Expression Kinetics from
782 Living Bacteria. Science *292*, 2080–2083.

783 Kieser, K.J., and Rubin, E.J. (2014). How sisters grow apart: mycobacterial growth and division.
784 Nat Rev Microbiol *12*, 550–562.

785 Kim, J.-H., Wei, J.-R., Wallach, J.B., Robbins, R.S., Rubin, E.J., and Schnappinger, D. (2011).
786 Protein inactivation in mycobacteria by controlled proteolysis and its application to deplete the
787 beta subunit of RNA polymerase. Nucleic Acids Research *39*, 2210–2220.

788 Kubitschek', H.E., and NEWMANt, C.N. (1978). Chromosome Replication During the Division
789 Cycle in Slowly Growing, Steady-State Cultures of Three Escherichia coli B/r Strains. *136*, 12.

790 Lark, K.G. (1961). Variation in bacterial acid-soluble deoxyribotides during discontinuous
791 deoxyribonucleic acid synthesis. Biochimica et Biophysica Acta *51*, 107–116.

792 Laub, M.T., McAdams, H.H., Feldblyum, T., Fraser, C.M., and Shapiro, L. (2000). Global Analysis
793 of the Genetic Network Controlling a Bacterial Cell Cycle. Science *290*, 2144–2148.

794 Lenarcic, R., Halbedel, S., Visser, L., Shaw, M., Wu, L.J., Errington, J., Marenduzzo, D., and
795 Hamoen, L.W. (2009). Localisation of DivIVA by targeting to negatively curved membranes.
796 EMBO J *28*, 2272–2282.

797 Li, H., and Durbin, R. (2009). Fast and accurate short read alignment with Burrows–Wheeler
798 transform. Bioinformatics *25*, 1754–1760.

799 Logsdon, M.M., and Aldridge, B.B. (2018). Stable Regulation of Cell Cycle Events in
800 Mycobacteria: Insights From Inherently Heterogeneous Bacterial Populations. Front. Microbiol.
801 514.

802 Logsdon, M.M., Ho, P.-Y., Papavinasasundaram, K., Richardson, K., Cokol, M., Sassetti, C.M.,
803 Amir, A., and Aldridge, B.B. (2017). A Parallel Adder Coordinates Mycobacterial Cell-Cycle
804 Progression and Cell-Size Homeostasis in the Context of Asymmetric Growth and Organization.
805 Current Biology *27*, 3367-3374.e7.

806 Love, M.I., Huber, W., and Anders, S. (2014). Moderated estimation of fold change and
807 dispersion for RNA-seq data with DESeq2. Genome Biol *15*.

808 Meniche, X., Otten, R., Siegrist, M.S., Baer, C.E., Murphy, K.C., Bertozzi, C.R., and Sassetti, C.M.
809 (2014). Subpolar addition of new cell wall is directed by DivIVA in mycobacteria. PNAS *111*,
810 E3243–E3251.

811 Mukherjee, A., and Lutkenhaus, J. (1998). Dynamic assembly of FtsZ regulated by GTP
812 hydrolysis. The EMBO Journal *17*, 462–469.

813 Nair, N., Dziedzic, R., Greendyke, R., Muniruzzaman, S., Rajagopalan, M., and Madiraju, M.V.
814 (2009). Synchronous replication initiation in novel Mycobacterium tuberculosis dnaA cold-
815 sensitive mutants. Molecular Microbiology *71*, 291–304.

816 Plocinska, R., Purushotham, G., Sarva, K., Vadrevu, I.S., Pandeeti, E.V.P., Arora, N., Plocinski, P.,
817 Madiraju, M.V., and Rajagopalan, M. (2012). Septal localization of the Mycobacterium

818 tuberculosis MtrB sensor kinase promotes MtrA regulon expression. J. Biol. Chem. *287*, 23887–
819 23899.

820 Ramamurthi, K.S., and Losick, R. (2009). Negative membrane curvature as a cue for subcellular
821 localization of a bacterial protein. PNAS *106*, 13541–13545.

822 Rego, E.H., Audette, R.E., and Rubin, E.J. (2017). Deletion of a mycobacterial divisome factor
823 collapses single-cell phenotypic heterogeneity. Nature *546*, 153–157.

824 Rock, J.M., Lang, U.F., Chase, M.R., Ford, C.B., Gerrick, E.R., Gawande, R., Coscolla, M., Gagneux,
825 S., Fortune, S.M., and Lamers, M.H. (2015). DNA replication fidelity in Mycobacterium
826 tuberculosis is mediated by an ancestral prokaryotic proofreader. Nat Genet *47*, 677–681.

827 Santi, I., and McKinney, J.D. (2015). Chromosome Organization and Replisome Dynamics in
828 Mycobacterium smegmatis. MBio *6*, e01999-14.

829 Santi, I., Dhar, N., Bousbaine, D., Wakamoto, Y., and McKinney, J.D. (2013). Single-cell dynamics
830 of the chromosome replication and cell division cycles in mycobacteria. Nat Commun *4*, 2470.

831 Sass, P., and Brötz-Oesterhelt, H. (2013). Bacterial cell division as a target for new antibiotics.
832 Current Opinion in Microbiology *16*, 522–530.

833 Sharma, A.K., Arora, D., Singh, L.K., Gangwal, A., Sajid, A., Molle, V., Singh, Y., and Nandicoori,
834 V.K. (2016). Serine/Threonine Protein Phosphatase PstP of *Mycobacterium tuberculosis* Is
835 Necessary for Accurate Cell Division and Survival of Pathogen. J. Biol. Chem. *291*, 24215–24230.

836 Singh, V., Donini, S., Pacitto, A., Sala, C., Hartkoorn, R.C., Dhar, N., Keri, G., Ascher, D.B.,
837 Mondésert, G., Vocat, A., et al. (2017). The Inosine Monophosphate Dehydrogenase, GuaB2, Is
838 a Vulnerable New Bactericidal Drug Target for Tuberculosis. ACS Infect. Dis. *3*, 5–17.

839 Skarstad, K., Steen, H.B., and Boye, E. (1983). Cell cycle parameters of slowly growing
840 Escherichia coli B/r studied by flow cytometry. J Bacteriol *154*, 656–662.

841 Trojanowski, D., Ginda, K., Pióro, M., Hołówka, J., Skut, P., Jakimowicz, D., and Zakrzewska-
842 Czerwińska, J. (2015). Choreography of the Mycobacterium Replication Machinery during the
843 Cell Cycle. MBio *6*, e02125-14.

844 Trojanowski, D., Hołówka, J., Ginda, K., Jakimowicz, D., and Zakrzewska-Czerwińska, J. (2017).
845 Multifork chromosome replication in slow-growing bacteria. Sci Rep *7*, 43836.

846 Vass, R.H., Zeinert, R.D., and Chien, P. (2016). Protease regulation and capacity during
847 Caulobacter growth. Current Opinion in Microbiology *34*, 75–81.

848 Wang, L., Khattar, M.K., Donachie, W.D., and Lutkenhaus, J. (1998). FtsI and FtsW Are Localized
849 to the Septum inEscherichia coli. Journal of Bacteriology *180*, 2810–2816.

Warner, D.F., Tønjum, T., and Mizrahi, V. (2013). DNA Metabolism in Mycobacterial Pathogenesis. Curr. Top. Microbiol. Immunol.

Weart, R.B., Lee, A.H., Chien, A.-C., Haeusser, D.P., Hill, N.S., and Levin, P.A. (2007). A Metabolic Sensor Governing Cell Size in Bacteria. Cell *130*, 335–347.

Wu, K.J., Zhang, J., Baranowski, C., Leung, V., Rego, E.H., Morita, Y.S., Rubin, E.J., and Boutte, C.C. (2018). Characterization of Conserved and Novel Septal Factors in Mycobacterium smegmatis. Journal of Bacteriology *200*.

Yaginuma, H., Kawai, S., Tabata, K.V., Tomiyama, K., Kakizuka, A., Komatsuzaki, T., Noji, H., and Imamura, H. (2015). Diversity in ATP concentrations in a single bacterial cell population revealed by quantitative single-cell imaging. Sci Rep *4*, 6522.

Zaslaver, A., Mayo, A.E., Rosenberg, R., Bashkin, P., Sberro, H., Tsalyuk, M., Surette, M.G., and Alon, U. (2004). Just-in-time transcription program in metabolic pathways. Nat Genet *36*, 486–491.

Zhang, Z., Milias-Argeitis, A., and Heinemann, M. (2018). Dynamic single-cell NAD(P)H measurement reveals oscillatory metabolism throughout the E. coli cell division cycle. Sci Rep *8*, 2162.

Acknowledgements

We would like to thank Aashish Srivastava under the guidance of James Sacchettini and the Texas A&M Genomics and Bioinformatics Service for sequencing the RNASeq libraries. VCC234718 was a generous gift from Vinayak Singh & Valerie Mizrahi. C109 was a generous gift from Vadim Makarov. Genetic depletion strains were generated as part of a larger collaborative effort including the labs of Deborah Hung, Eric Rubin, Sabine Ehrt and Dirk Schnappinger. Kenan Murphy and Charlotte Reames contributed to strain generation from the Sassetti lab. We would like to thank Megan Proulx for critical reading of the manuscript. This work was supported by grant AI095208 to CMS.

Author contributions

Conceptualization- ACB, TRI, CMS

Methodology- ACB, TRI

Investigation- ACB

Validation- ACB

Formal Analysis- ACB, SS, TRI

Writing Original Draft- ACB

Writing Review & Editing- ACB, TRI, CMS

Funding acquisition- CMS

Supervision- CMS

Declaration of interests

The authors declare no competing interests.

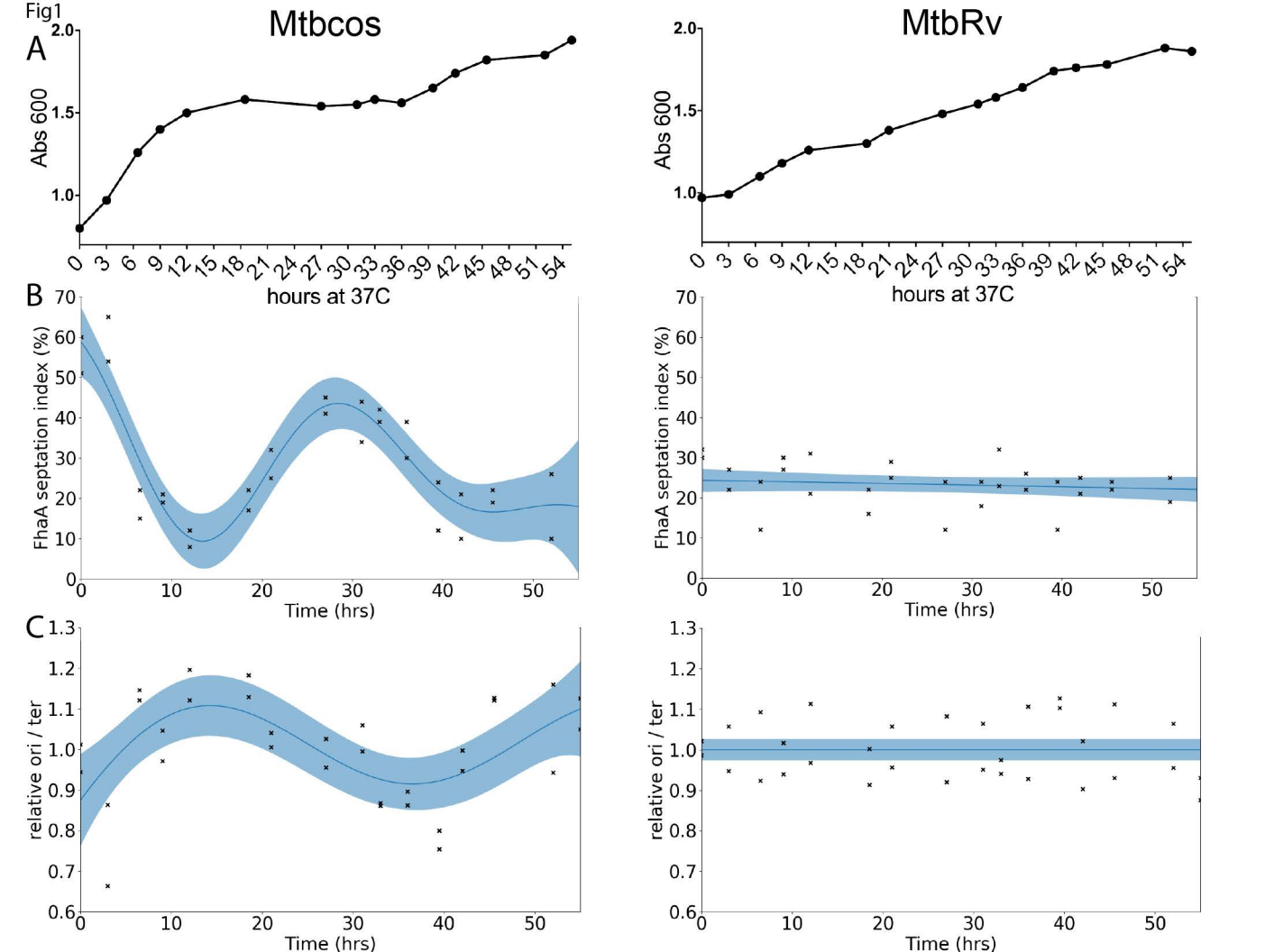
Fig1
A
Mtbcos
MtbRv
Abs 600
B
hours at 37C
FhaA septation index (%)
Time (hrs)
C
relative ori / ter

Fig 2

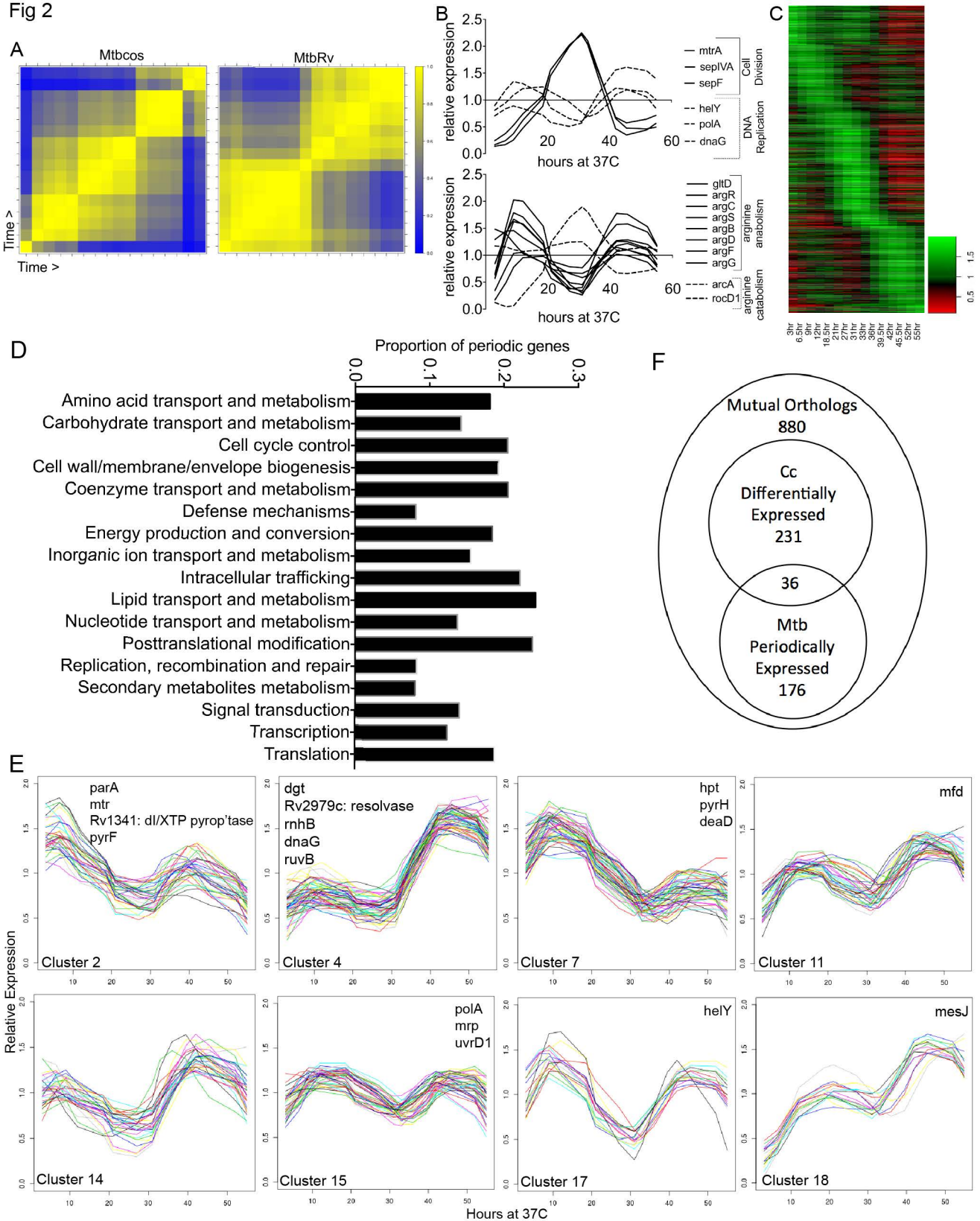
A
Mtbcos
MtbRv
Time >
Time >
B
relative expression
hours at 37C
mtrA
sepIVA
sepF
Cell Division
helY
polA
dnaG
DNA Replication
gltD
argR
argC
argJ
argB
argD
argF
argG
arginine anabolism
arcA
rocD1
arginine catabolism
C
3hr
6.5hr
9hr
12hr
18.5hr
21hr
27hr
31hr
33hr
36hr
39.5hr
42hr
45.5hr
52hr
55hr
D
Proportion of periodic genes
Amino acid transport and metabolism
Carbohydrate transport and metabolism
Cell cycle control
Cell wall/membrane/envelope biogenesis
Coenzyme transport and metabolism
Defense mechanisms
Energy production and conversion
Inorganic ion transport and metabolism
Intracellular trafficking
Lipid transport and metabolism
Nucleotide transport and metabolism
Posttranslational modification
Replication, recombination and repair
Secondary metabolites metabolism
Signal transduction
Transcription
Translation
F
Mutual Orthologs
880
Cc
Differentially
Expressed
231
36
Mtb
Periodically
Expressed
176
E
parA
mtr
Rv1341: dI/XTP pyrop'tase
pyrF
Cluster 2
dgt
Rv2979c: resolvase
rnhB
dnaG
ruvB
Cluster 4
hpt
pyrH
deaD
Cluster 7
mfd
Cluster 11
Relative Expression
polA
mrp
uvrD1
Cluster 14
Cluster 15
helY
Cluster 17
mesJ
Cluster 18
Hours at 37C

Fig 3

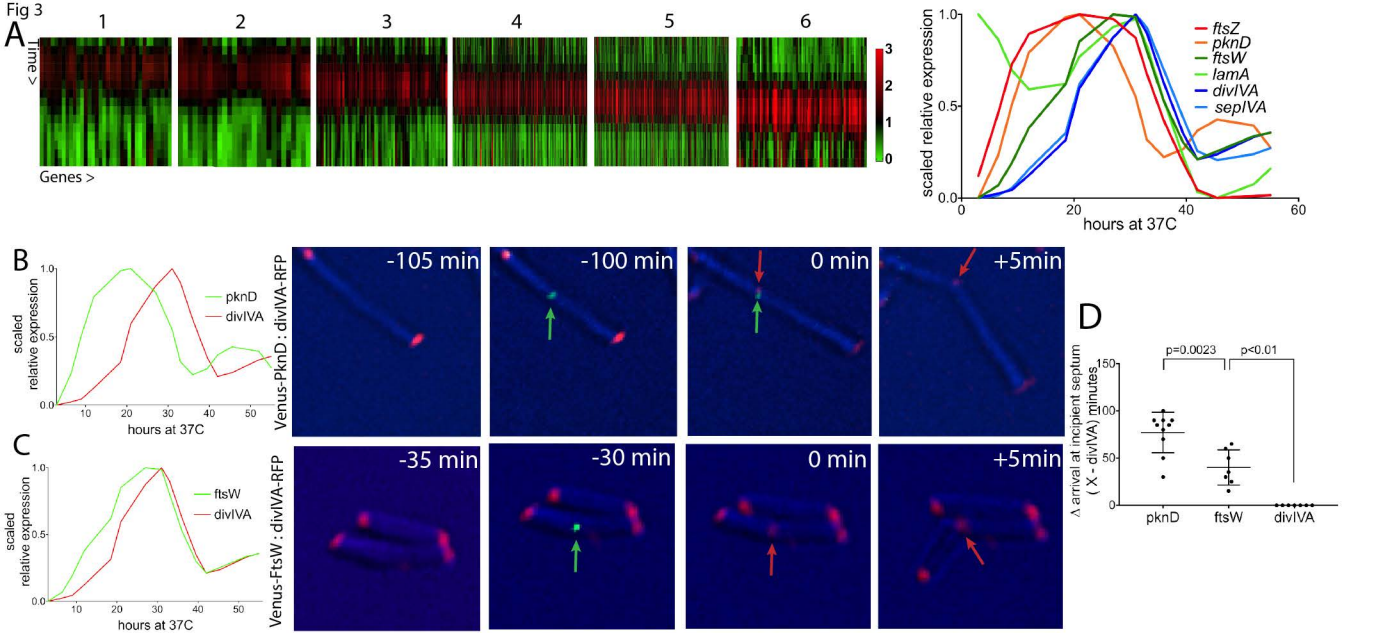
A
1
2
3
4
5
6
Genes >
3
2
1
0
scaled relative expression
1.0
0.5
0.0
0
20
40
60
hours at 37C
ftsZ
pknD
ftsW
lamA
divIVA
sepIVA
B
scaled relative expression
pknD
divIVA
hours at 37C
Venus-PknD : divIVA-RFP
-105 min
-100 min
0 min
+5min
C
scaled relative expression
ftsW
divIVA
hours at 37C
Venus-FtsW : divIVA-RFP
-35 min
-30 min
0 min
+5min
D
p=0.0023
p<0.01
Δ arrival at incipient septum (X - divIVA) minutes
150
100
50
0
pknD
ftsW
divIVA

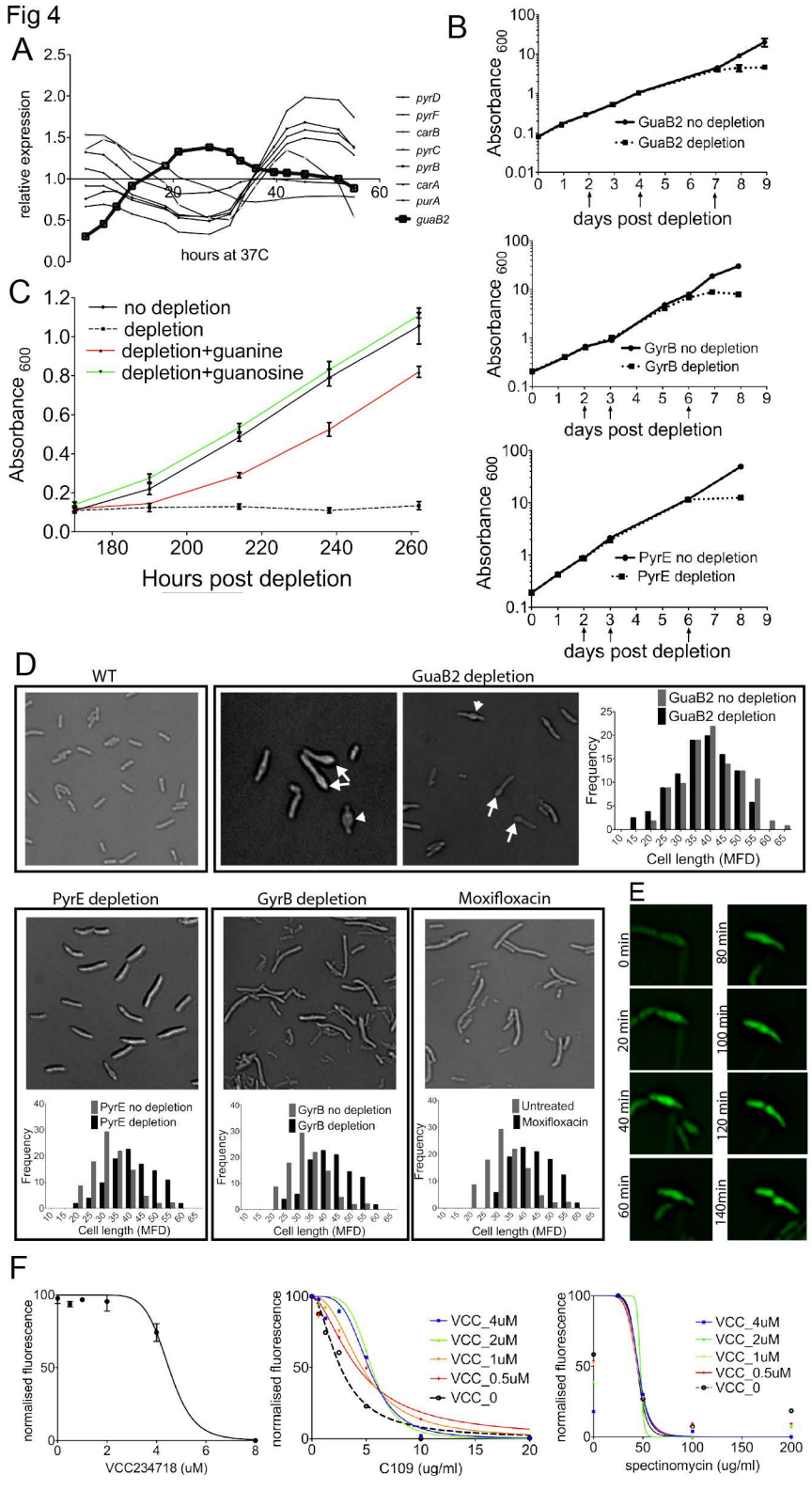
Fig 4
A
relative expression
hours at 37C
pyrD
pyrF
carB
pyrC
pyrB
carA
purA
guaB2
B
Absorbance 600
GuaB2 no depletion
GuaB2 depletion
days post depletion
GyrB no depletion
GyrB depletion
PyrE no depletion
PyrE depletion
C
no depletion
depletion
depletion+guanine
depletion+guanosine
Hours post depletion
D
WT
GuaB2 depletion
Frequency
Cell length (MFD)
PyrE depletion
GyrB depletion
Moxifloxacin
Untreated
E
0 min
20 min
40 min
60 min
80 min
100 min
120 min
140min
F
normalised fluorescence
VCC234718 (uM)
C109 (ug/ml)
spectinomycin (ug/ml)
VCC_4uM
VCC_2uM
VCC_1uM
VCC_0.5uM
VCC_0

Fig S1

A

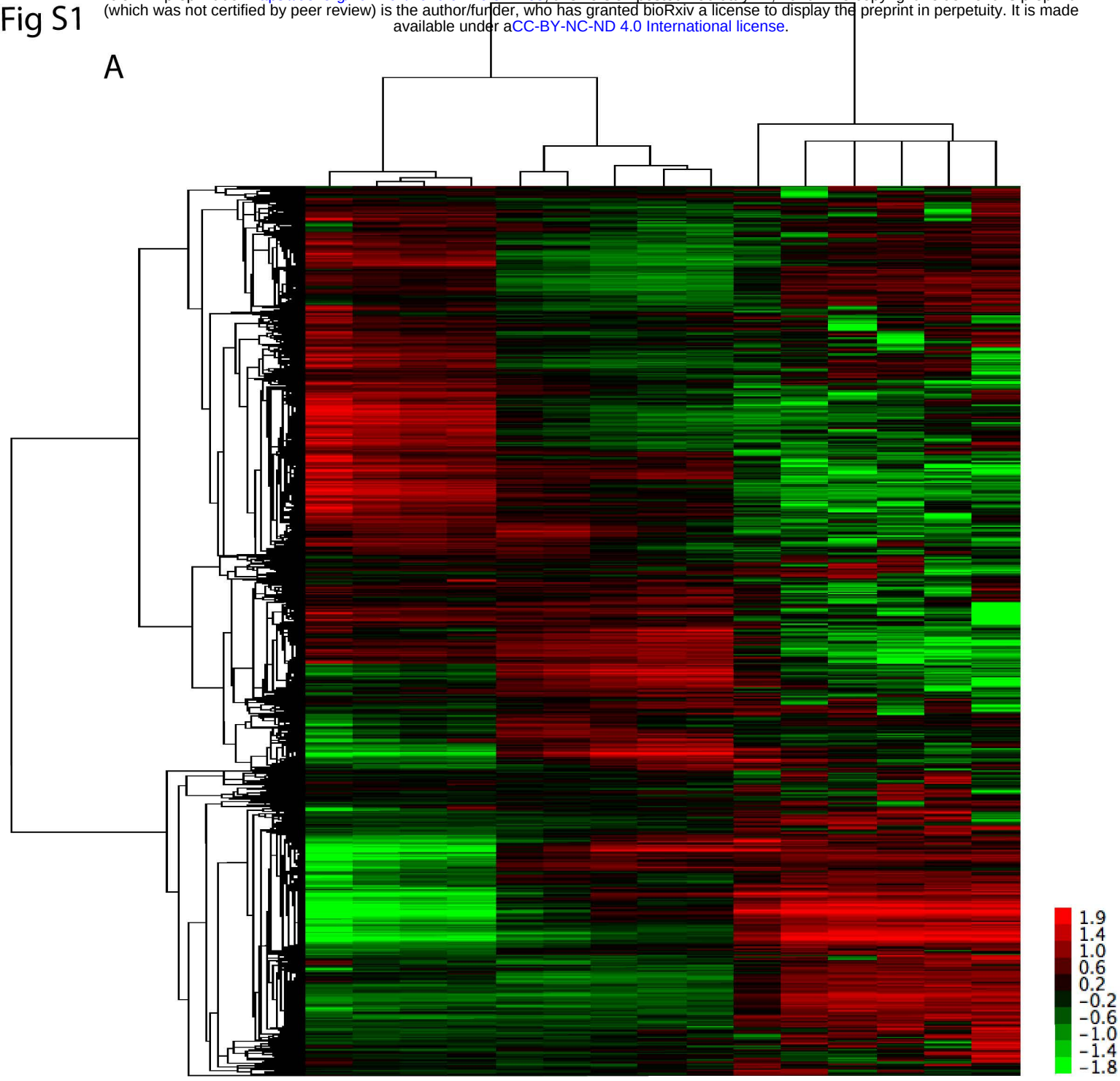

B

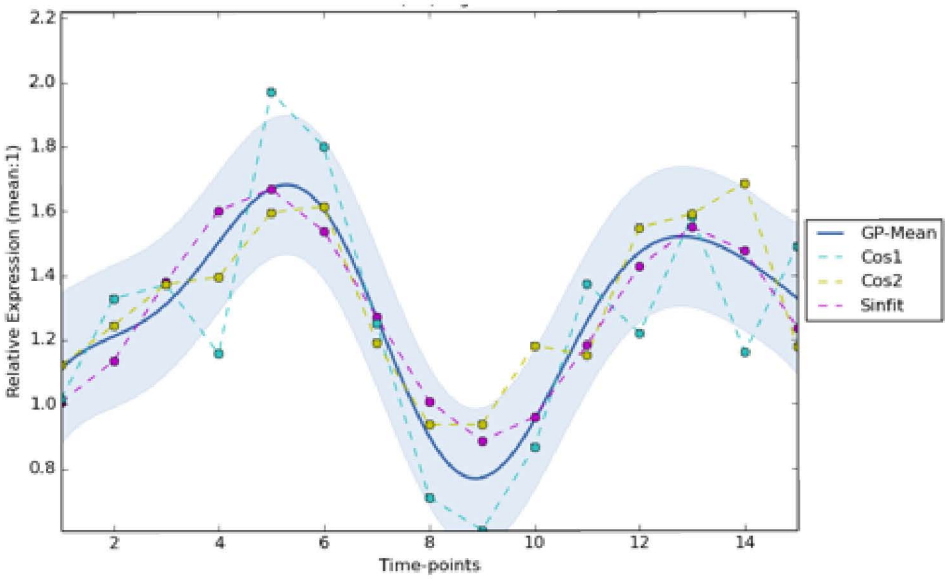

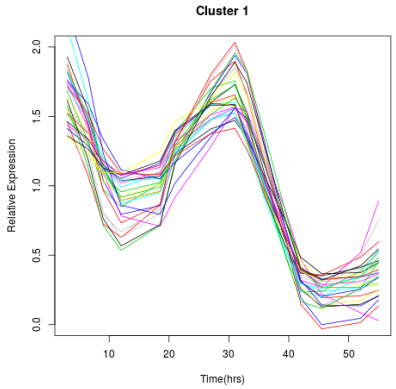
Cluster 1
Relative Expression
0.0
0.5
1.0
1.5
2.0
10
20
30
40
50
Time(hrs)

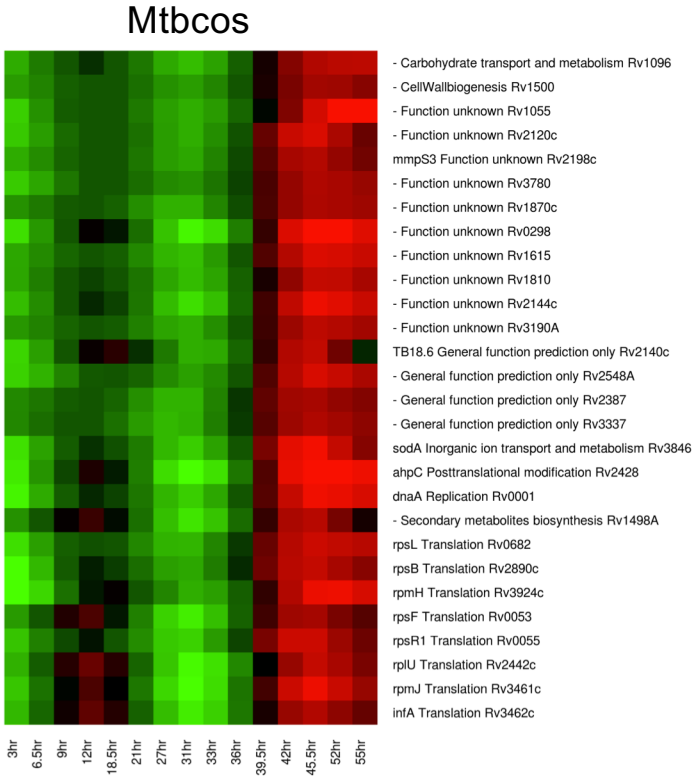
Mtbcos
- Carbohydrate transport and metabolism Rv1096
- CellWallbiogenesis Rv1500
- Function unknown Rv1055
- Function unknown Rv2120c
mmpS3 Function unknown Rv2198c
- Function unknown Rv3780
- Function unknown Rv1870c
- Function unknown Rv0298
- Function unknown Rv1615
- Function unknown Rv1810
- Function unknown Rv2144c
- Function unknown Rv3190A
TB18.6 General function prediction only Rv2140c
- General function prediction only Rv2548A
- General function prediction only Rv2387
- General function prediction only Rv3337
sodA Inorganic ion transport and metabolism Rv3846
ahpC Posttranslational modification Rv2428
dnaA Replication Rv0001
- Secondary metabolites biosynthesis Rv1498A
rpsL Translation Rv0682
rpsB Translation Rv2890c
rpmH Translation Rv3924c
rpsF Translation Rv0053
rpsR1 Translation Rv0055
rplU Translation Rv2442c
rpmJ Translation Rv3461c
infA Translation Rv3462c
3hr
6.5hr
9hr
12hr
18.5hr
21hr
27hr
31hr
33hr
36hr
39.5hr
42hr
45.5hr
52hr
55hr

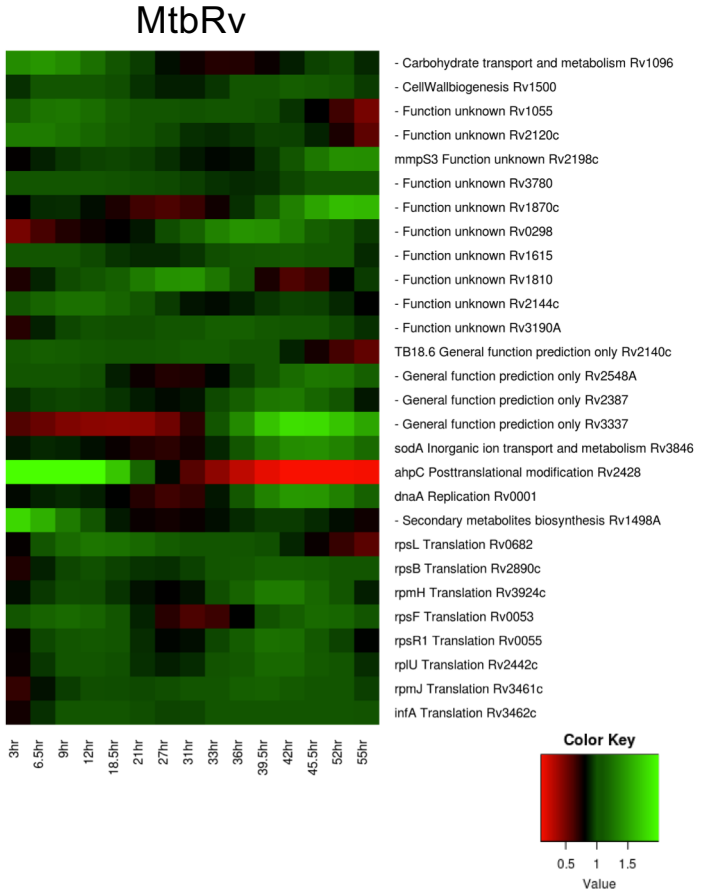
MtbRv
- Carbohydrate transport and metabolism Rv1096
- CellWallbiogenesis Rv1500
- Function unknown Rv1055
- Function unknown Rv2120c
mmpS3 Function unknown Rv2198c
- Function unknown Rv3780
- Function unknown Rv1870c
- Function unknown Rv0298
- Function unknown Rv1615
- Function unknown Rv1810
- Function unknown Rv2144c
- Function unknown Rv3190A
TB18.6 General function prediction only Rv2140c
- General function prediction only Rv2548A
- General function prediction only Rv2387
- General function prediction only Rv3337
sodA Inorganic ion transport and metabolism Rv3846
ahpC Posttranslational modification Rv2428
dnaA Replication Rv0001
- Secondary metabolites biosynthesis Rv1498A
rpsL Translation Rv0682
rpsB Translation Rv2890c
rpmH Translation Rv3924c
rpsF Translation Rv0053
rpsR1 Translation Rv0055
rplU Translation Rv2442c
rpmJ Translation Rv3461c
infA Translation Rv3462c
3hr
6.5hr
9hr
12hr
18.5hr
21hr
27hr
31hr
33hr
36hr
39.5hr
42hr
45.5hr
52hr
55hr
Color Key
0.5
1
1.5
Value

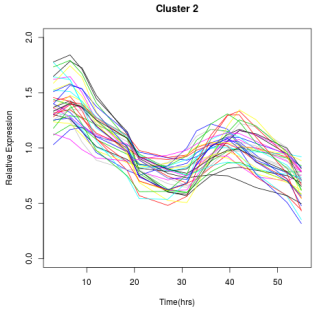

Mtbcos

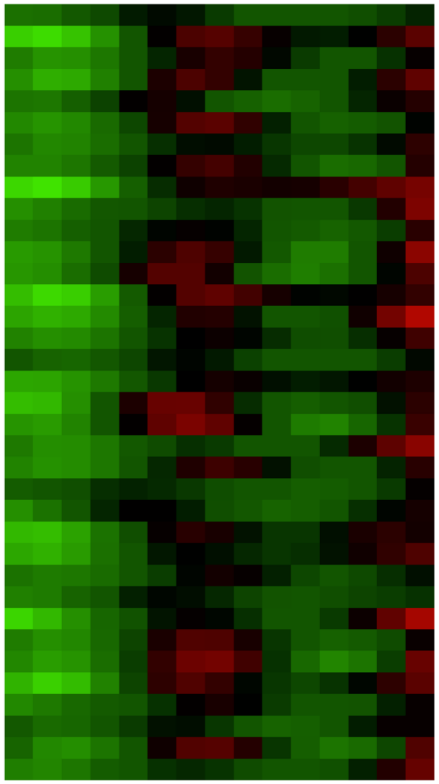

3hr 6.5hr 9hr 12hr 18.5hr 21hr 27hr 31hr 33hr 36hr 39.5hr 42hr 45.5hr 52hr 55hr

- Amino acid transport and metabolism Rv2690c
ppnK Carbohydrate transport and metabolism Rv1695
rodA Cell cycle control Rv0017c
parA Cell cycle control Rv3918c
lpqU CellWallbiogenesis Rv1022
epiA CellWallbiogenesis Rv1512
ribF Coenzyme transport and metabolism Rv2786c
galTa Energy production and conversion Rv0618
mtr Energy production and conversion Rv2855
- Function unknown Rv0039c
- Function unknown Rv0625c
- Function unknown Rv3770B
- Function unknown Rv3906c
- Function unknown Rv0007
- Function unknown Rv3355c
- Function unknown Rv3695
eccE5 Function unknown Rv1797
- General function prediction only Rv2223c
- General function prediction only Rv3362c
- General function prediction only Rv0804
mmpL12 General function prediction only Rv1522c
- General function prediction only Rv3677c
- General function prediction only Rv3376
secG Intracellular trafficking Rv1440
- Lipid transport and metabolism Rv0517
menE Lipid transport and metabolism Rv0542c
- Lipid transport and metabolism Rv0945
purA Nucleotide transport and metabolism Rv0357c
- Nucleotide transport and metabolism Rv1262c
- Nucleotide transport and metabolism Rv1341
pyrF Nucleotide transport and metabolism Rv1385
- Replication Rv3431c
orn RNA processing and modification Rv2511
- Transcription Rv0023
sigJ Transcription Rv3328c
- Translation Rv3300c

MtbRv

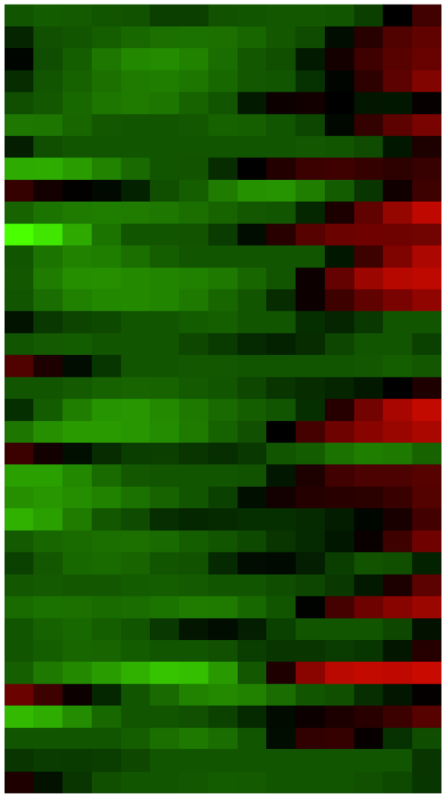

3hr 6.5hr 9hr 12hr 18.5hr 21hr 27hr 31hr 33hr 36hr 39.5hr 42hr 45.5hr 52hr 55hr

- Amino acid transport and metabolism Rv2690c
ppnK Carbohydrate transport and metabolism Rv1695
rodA Cell cycle control Rv0017c
parA Cell cycle control Rv3918c
lpqU CellWallbiogenesis Rv1022
epiA CellWallbiogenesis Rv1512
ribF Coenzyme transport and metabolism Rv2786c
galTa Energy production and conversion Rv0618
mtr Energy production and conversion Rv2855
- Function unknown Rv0039c
- Function unknown Rv0625c
- Function unknown Rv3770B
- Function unknown Rv3906c
- Function unknown Rv0007
- Function unknown Rv3355c
- Function unknown Rv3695
eccE5 Function unknown Rv1797
- General function prediction only Rv2223c
- General function prediction only Rv3362c
- General function prediction only Rv0804
mmpL12 General function prediction only Rv1522c
- General function prediction only Rv3677c
- General function prediction only Rv3376
secG Intracellular trafficking Rv1440
- Lipid transport and metabolism Rv0517
menE Lipid transport and metabolism Rv0542c
- Lipid transport and metabolism Rv0945
purA Nucleotide transport and metabolism Rv0357c
- Nucleotide transport and metabolism Rv1262c
- Nucleotide transport and metabolism Rv1341
pyrF Nucleotide transport and metabolism Rv1385
- Replication Rv3431c
orn RNA processing and modification Rv2511
- Transcription Rv0023
sigJ Transcription Rv3328c
- Translation Rv3300c

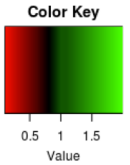

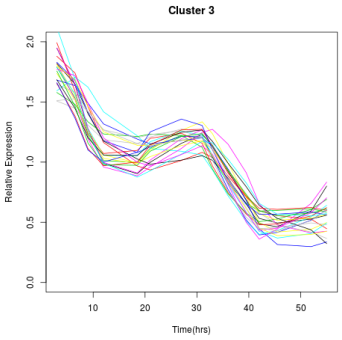
Cluster 3
Relative Expression
0.0
0.5
1.0
1.5
2.0
10
20
30
40
50
Time(hrs)

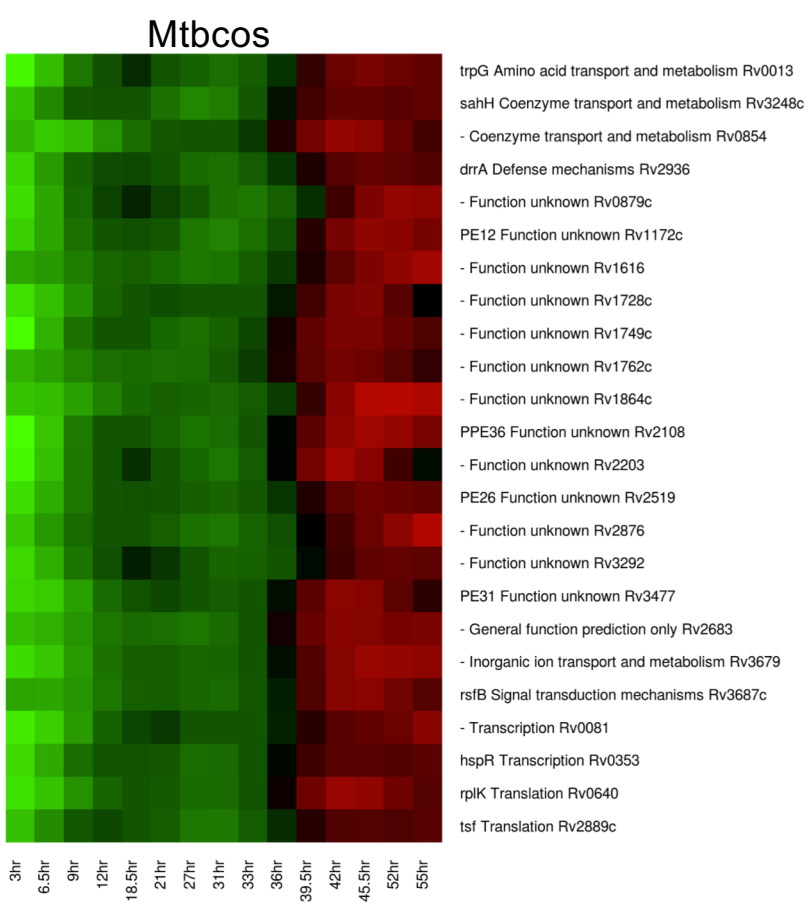
Mtbcos
trpG Amino acid transport and metabolism Rv0013
sahH Coenzyme transport and metabolism Rv3248c
- Coenzyme transport and metabolism Rv0854
drrA Defense mechanisms Rv2936
- Function unknown Rv0879c
PE12 Function unknown Rv1172c
- Function unknown Rv1616
- Function unknown Rv1728c
- Function unknown Rv1749c
- Function unknown Rv1762c
- Function unknown Rv1864c
PPE36 Function unknown Rv2108
- Function unknown Rv2203
PE26 Function unknown Rv2519
- Function unknown Rv2876
- Function unknown Rv3292
PE31 Function unknown Rv3477
- General function prediction only Rv2683
- Inorganic ion transport and metabolism Rv3679
rsfB Signal transduction mechanisms Rv3687c
- Transcription Rv0081
hspR Transcription Rv0353
rplK Translation Rv0640
tsf Translation Rv2889c
3hr
6.5hr
9hr
12hr
18.5hr
21hr
27hr
31hr
33hr
36hr
39.5hr
42hr
45.5hr
52hr
55hr

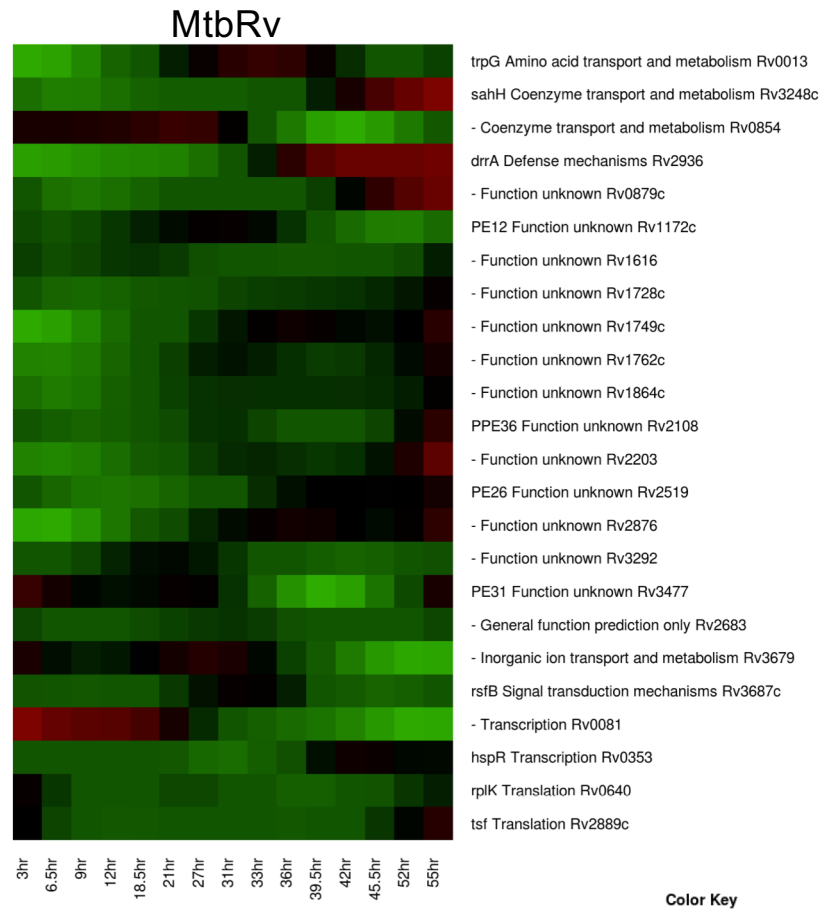
MtbRv
trpG Amino acid transport and metabolism Rv0013
sahH Coenzyme transport and metabolism Rv3248c
- Coenzyme transport and metabolism Rv0854
drrA Defense mechanisms Rv2936
- Function unknown Rv0879c
PE12 Function unknown Rv1172c
- Function unknown Rv1616
- Function unknown Rv1728c
- Function unknown Rv1749c
- Function unknown Rv1762c
- Function unknown Rv1864c
PPE36 Function unknown Rv2108
- Function unknown Rv2203
PE26 Function unknown Rv2519
- Function unknown Rv2876
- Function unknown Rv3292
PE31 Function unknown Rv3477
- General function prediction only Rv2683
- Inorganic ion transport and metabolism Rv3679
rsfB Signal transduction mechanisms Rv3687c
- Transcription Rv0081
hspR Transcription Rv0353
rplK Translation Rv0640
tsf Translation Rv2889c
3hr
6.5hr
9hr
12hr
18.5hr
21hr
27hr
31hr
33hr
36hr
39.5hr
42hr
45.5hr
52hr
55hr


Color Key
0.5
1
1.5
Value

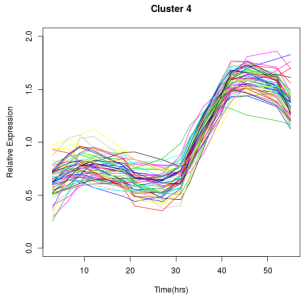

Mtbcos

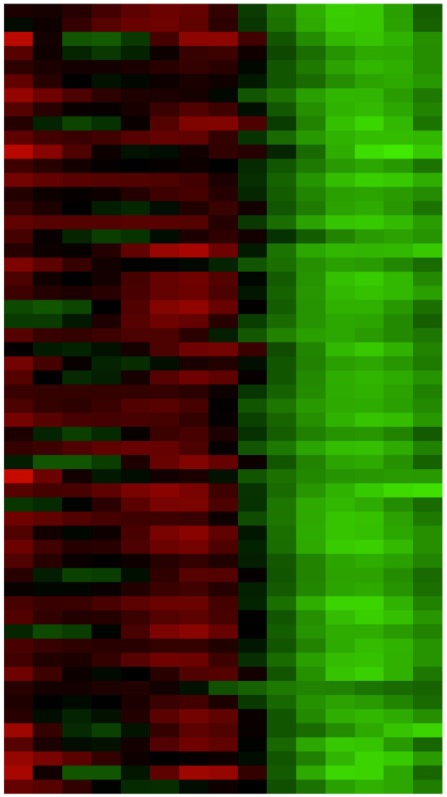

- Amino acid transport and metabolism Rv0492c
lpqW Amino acid transport and metabolism Rv1166
argJ Amino acid transport and metabolism Rv1653
aroK Amino acid transport and metabolism Rv2539c
aroA Amino acid transport and metabolism Rv3227
pheA Amino acid transport and metabolism Rv3838c
glgB Carbohydrate transport and metabolism Rv1326c
pdc Carbohydrate transport and metabolism Rv0853c
menC CellWallbiogenesis Rv0553
- CellWallbiogenesis Rv0024
- CellWallbiogenesis Rv1478
hemD Coenzyme transport and metabolism Rv0511
menH Coenzyme transport and metabolism Rv0558
fbiC Coenzyme transport and metabolism Rv1173
folC Coenzyme transport and metabolism Rv2447c
folD Coenzyme transport and metabolism Rv3356c
hemB Coenzyme transport and metabolism Rv0512
lipP Defense mechanisms Rv2463
citA Energy production and conversion Rv0889c
ackA Energy production and conversion Rv0409
- Energy production and conversion Rv0561c
lpdA Energy production and conversion Rv3303c
PPE42 Function unknown Rv2608
- Function unknown Rv3770c
- Function unknown Rv1312
- Function unknown Rv2345
- Function unknown Rv2474c
- Function unknown Rv2732c
- Function unknown Rv3091
PE_PGRS59 Function unknown Rv3595c
lpqG Function unknown Rv3623
- Function unknown Rv3658c
- Function unknown Rv3909
- Function unknown Rv2033c
PE_PGRS24 Function unknown Rv1325c
- General function prediction only Rv1204c
- General function prediction only Rv1770
- General function prediction only Rv2475c
- General function prediction only Rv0552
- General function prediction only Rv2314c
- General function prediction only Rv3510c
ffh Intracellular trafficking Rv2916c
fadE2 Lipid transport and metabolism Rv0154c
fadA2 Lipid transport and metabolism Rv0243
echA9 Lipid transport and metabolism Rv1071c
dgt Nucleotide transport and metabolism Rv2344c
mycP5 Posttranslational modification Rv1796
- Posttranslational modification Rv3421c
- Replication Rv2979c
rnhB Replication Rv2902c
dnaG Replication Rv2343c
ruvB Replication Rv2592c
devS Signal transduction mechanisms Rv3132c
trcR Signal transduction mechanisms Rv1033c
argR Transcription Rv1657
valS Translation Rv2448c

3hr 6.5hr 9hr 12hr 18.5hr 21hr 27hr 31hr 33hr 36hr 39.5hr 42hr 45.5hr 52hr 55hr

MtbRv

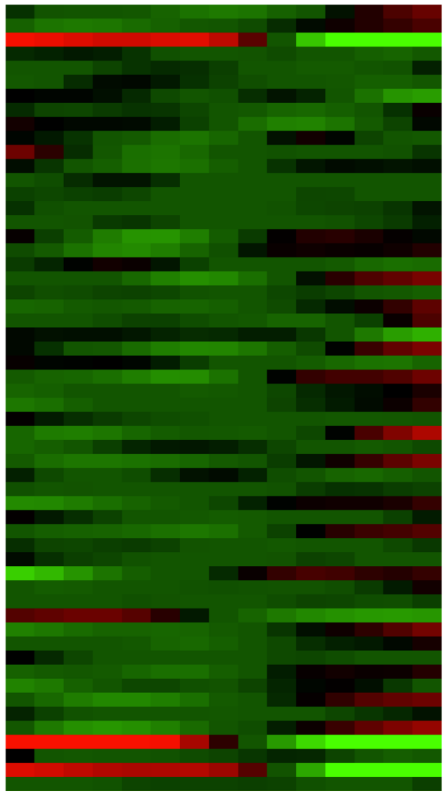

- Amino acid transport and metabolism Rv0492c
lpqW Amino acid transport and metabolism Rv1166
argJ Amino acid transport and metabolism Rv1653
aroK Amino acid transport and metabolism Rv2539c
aroA Amino acid transport and metabolism Rv3227
pheA Amino acid transport and metabolism Rv3838c
glgB Carbohydrate transport and metabolism Rv1326c
pdc Carbohydrate transport and metabolism Rv0853c
menC CellWallbiogenesis Rv0553
- CellWallbiogenesis Rv0024
- CellWallbiogenesis Rv1478
hemD Coenzyme transport and metabolism Rv0511
menH Coenzyme transport and metabolism Rv0558
fbiC Coenzyme transport and metabolism Rv1173
folC Coenzyme transport and metabolism Rv2447c
folD Coenzyme transport and metabolism Rv3356c
hemB Coenzyme transport and metabolism Rv0512
lipP Defense mechanisms Rv2463
citA Energy production and conversion Rv0889c
ackA Energy production and conversion Rv0409
- Energy production and conversion Rv0561c
lpdA Energy production and conversion Rv3303c
PPE42 Function unknown Rv2608
- Function unknown Rv3770c
- Function unknown Rv1312
- Function unknown Rv2345
- Function unknown Rv2474c
- Function unknown Rv2732c
- Function unknown Rv3091
PE_PGRS59 Function unknown Rv3595c
lpqG Function unknown Rv3623
- Function unknown Rv3658c
- Function unknown Rv3909
- Function unknown Rv2033c
PE_PGRS24 Function unknown Rv1325c
- General function prediction only Rv1204c
- General function prediction only Rv1770
- General function prediction only Rv2475c
- General function prediction only Rv0552
- General function prediction only Rv2314c
- General function prediction only Rv3510c
ffh Intracellular trafficking Rv2916c
fadE2 Lipid transport and metabolism Rv0154c
fadA2 Lipid transport and metabolism Rv0243
echA9 Lipid transport and metabolism Rv1071c
dgt Nucleotide transport and metabolism Rv2344c
mycP5 Posttranslational modification Rv1796
- Posttranslational modification Rv3421c
- Replication Rv2979c
rnhB Replication Rv2902c
dnaG Replication Rv2343c
ruvB Replication Rv2592c
devS Signal transduction mechanisms Rv3132c
trcR Signal transduction mechanisms Rv1033c
argR Transcription Rv1657
valS Translation Rv2448c

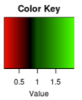

3hr 6.5hr 9hr 12hr 18.5hr 21hr 27hr 31hr 33hr 36hr 39.5hr 42hr 45.5hr 52hr 55hr

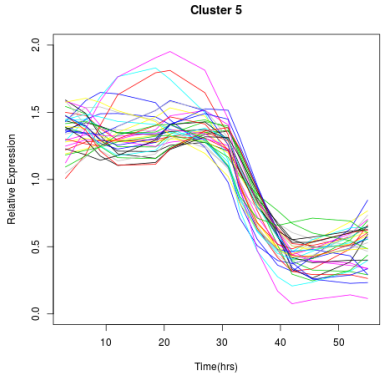

Mtbcos

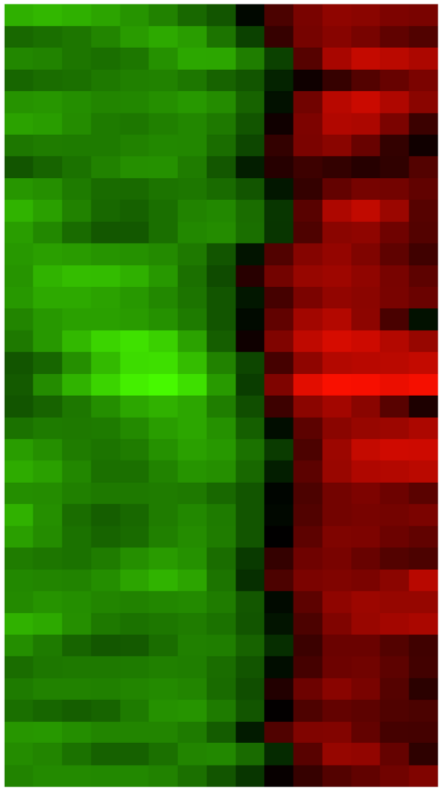

- Amino acid transport and metabolism Rv3684
hisA Amino acid transport and metabolism Rv1603
glnA2 Amino acid transport and metabolism Rv2222c
- Carbohydrate transport and metabolism Rv3075c
lipA Coenzyme transport and metabolism Rv2218
icd2 Energy production and conversion Rv0066c
gpdA1 Energy production and conversion Rv0564c
glpQ1 Energy production and conversion Rv3842c
- Function unknown Rv0025
- Function unknown Rv0909
- Function unknown Rv3822
esxP Function unknown Rv2347c
- Function unknown Rv0349
- Function unknown Rv1871c
- Function unknown Rv1269c
- Function unknown Rv0463
- Function unknown Rv2175c
- Function unknown Rv3612c
- Function unknown Rv3705A
- Function unknown Rv0543c
espR Function unknown Rv3849
- General function prediction only Rv0229c
- General function prediction only Rv2581c
- General function prediction only Rv2716
- General function prediction only Rv3338
adhC General function prediction only Rv3045
- General function prediction only Rv3284
tatA Intracellular trafficking Rv2094c
fadD25 Lipid transport and metabolism Rv1521
fadD32 Lipid transport and metabolism Rv3801c
fadD14 Lipid transport and metabolism Rv1058
- Lipid transport and metabolism Rv2361c
fadD28 Lipid transport and metabolism Rv2941
- Posttranslational modification Rv1324
pks3 Secondary metabolites biosynthesis Rv1180
yrbE2B Secondary metabolites biosynthesis Rv0588

MtbRv

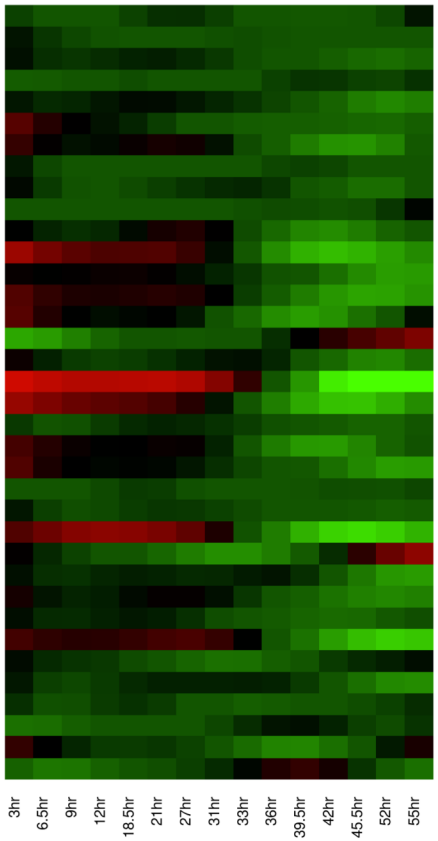

- Amino acid transport and metabolism Rv3684
hisA Amino acid transport and metabolism Rv1603
glnA2 Amino acid transport and metabolism Rv2222c
- Carbohydrate transport and metabolism Rv3075c
lipA Coenzyme transport and metabolism Rv2218
icd2 Energy production and conversion Rv0066c
gpdA1 Energy production and conversion Rv0564c
glpQ1 Energy production and conversion Rv3842c
- Function unknown Rv0025
- Function unknown Rv0909
- Function unknown Rv3822
esxP Function unknown Rv2347c
- Function unknown Rv0349
- Function unknown Rv1871c
- Function unknown Rv1269c
- Function unknown Rv0463
- Function unknown Rv2175c
- Function unknown Rv3612c
- Function unknown Rv3705A
- Function unknown Rv0543c
espR Function unknown Rv3849
- General function prediction only Rv0229c
- General function prediction only Rv2581c
- General function prediction only Rv2716
- General function prediction only Rv3338
adhC General function prediction only Rv3045
- General function prediction only Rv3284
tatA Intracellular trafficking Rv2094c
fadD25 Lipid transport and metabolism Rv1521
fadD32 Lipid transport and metabolism Rv3801c
fadD14 Lipid transport and metabolism Rv1058
- Lipid transport and metabolism Rv2361c
fadD28 Lipid transport and metabolism Rv2941
- Posttranslational modification Rv1324
pks3 Secondary metabolites biosynthesis Rv1180
yrbE2B Secondary metabolites biosynthesis Rv0588

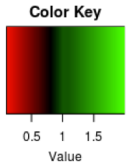

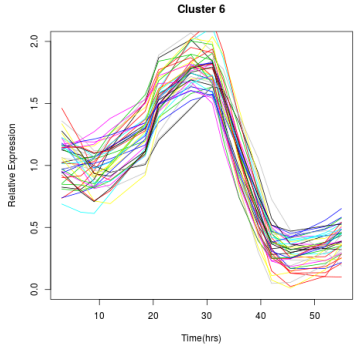

Mtbcos

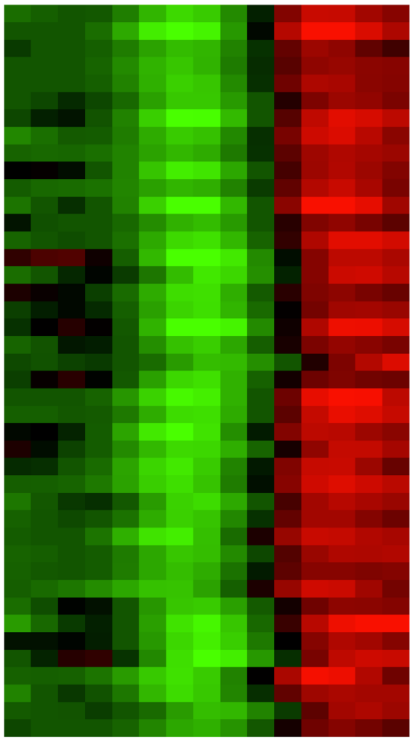

3hr 6.5hr 9hr 12hr 18.5hr 21hr 27hr 31hr 33hr 36hr 39.5hr 42hr 45.5hr 52hr 55hr

hisB Amino acid transport and metabolism Rv1601
glnB Amino acid transport and metabolism Rv2919c
- CellWallbiogenesis Rv2721c
fdxC Energy production and conversion Rv1177
- Function unknown Rv0027
vapB31 Function unknown Rv0748
- Function unknown Rv0863
- Function unknown Rv1261c
esxN Function unknown Rv1793
- Function unknown Rv2632c
- Function unknown Rv3190c
- Function unknown Rv3528c
- Function unknown Rv0426c
- Function unknown Rv0559c
- Function unknown Rv0686
- Function unknown Rv0755A
- Function unknown Rv1072
- Function unknown Rv1211
pup Function unknown Rv2111c
whiB1 Function unknown Rv3219
- Function unknown Rv3642c
- Function unknown Rv3675
vapC2 General function prediction only Rv0301
vapB48 General function prediction only Rv3697A
cysA2 Inorganic ion transport and metabolism Rv0815c
phoY2 Inorganic ion transport and metabolism Rv0821c
cysA3 Inorganic ion transport and metabolism Rv3117
sseA Inorganic ion transport and metabolism Rv3283
- Inorganic ion transport and metabolism Rv3049c
fadE20 Lipid transport and metabolism Rv2724c
fadE24 Lipid transport and metabolism Rv3139
prcB Posttranslational modification Rv2110c
- Secondary metabolites biosynthesis Rv1978
ephG Secondary metabolites biosynthesis Rv2740
- Secondary metabolites biosynthesis Rv0726c
lprD Transcription Rv1343c
- Transcription Rv1404
parD1 Transcription Rv1960c
relE Translation Rv1246c
frr Translation Rv2882c
rpmE Translation Rv1298
ileS Translation Rv1536

MtbRv

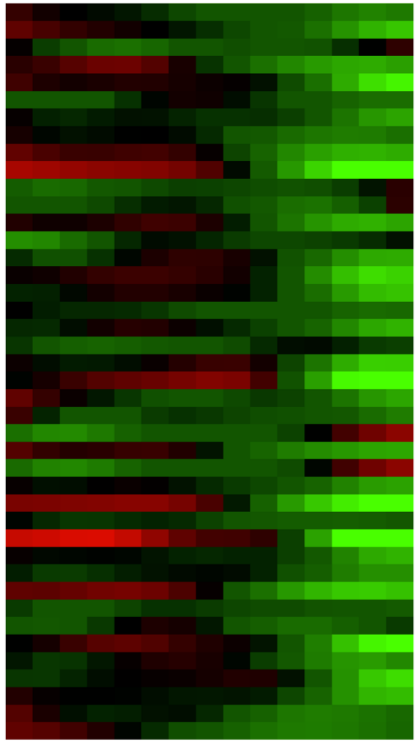

3hr 6.5hr 9hr 12hr 18.5hr 21hr 27hr 31hr 33hr 36hr 39.5hr 42hr 45.5hr 52hr 55hr

hisB Amino acid transport and metabolism Rv1601
glnB Amino acid transport and metabolism Rv2919c
- CellWallbiogenesis Rv2721c
fdxC Energy production and conversion Rv1177
- Function unknown Rv0027
vapB31 Function unknown Rv0748
- Function unknown Rv0863
- Function unknown Rv1261c
esxN Function unknown Rv1793
- Function unknown Rv2632c
- Function unknown Rv3190c
- Function unknown Rv3528c
- Function unknown Rv0426c
- Function unknown Rv0559c
- Function unknown Rv0686
- Function unknown Rv0755A
- Function unknown Rv1072
- Function unknown Rv1211
pup Function unknown Rv2111c
whiB1 Function unknown Rv3219
- Function unknown Rv3642c
- Function unknown Rv3675
vapC2 General function prediction only Rv0301
vapB48 General function prediction only Rv3697A
cysA2 Inorganic ion transport and metabolism Rv0815c
phoY2 Inorganic ion transport and metabolism Rv0821c
cysA3 Inorganic ion transport and metabolism Rv3117
sseA Inorganic ion transport and metabolism Rv3283
- Inorganic ion transport and metabolism Rv3049c
fadE20 Lipid transport and metabolism Rv2724c
fadE24 Lipid transport and metabolism Rv3139
prcB Posttranslational modification Rv2110c
- Secondary metabolites biosynthesis Rv1978
ephG Secondary metabolites biosynthesis Rv2740
- Secondary metabolites biosynthesis Rv0726c
lprD Transcription Rv1343c
- Transcription Rv1404
parD1 Transcription Rv1960c
relE Translation Rv1246c
frr Translation Rv2882c
rpmE Translation Rv1298
ileS Translation Rv1536

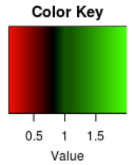

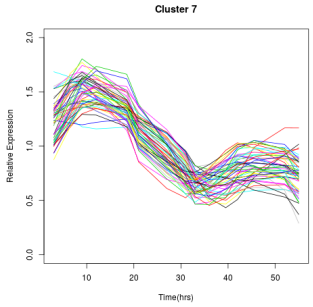

Mtbcos

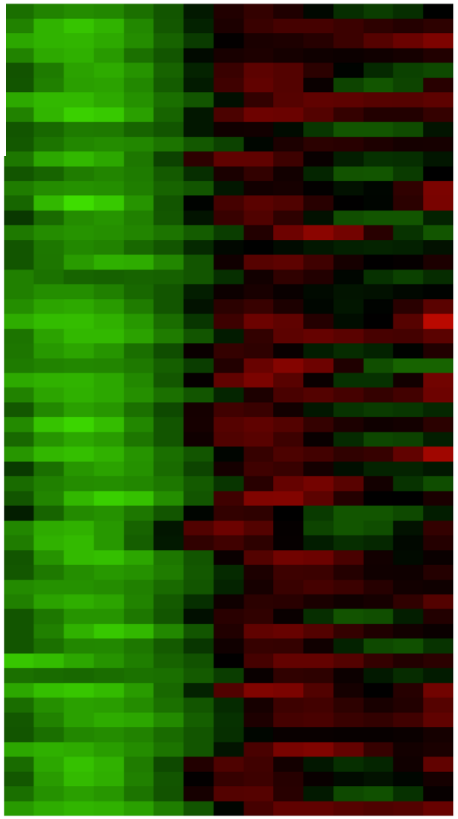

3hr 6.5hr 9hr 12hr 18.5hr 21hr 27hr 31hr 33hr 36hr 39.5hr 42hr 45.5hr 52hr 55hr

- Amino acid transport and metabolism Rv1413
- Amino acid transport and metabolism Rv1769
- Amino acid transport and metabolism Rv2409c
proA Amino acid transport and metabolism Rv2427c
proZ Amino acid transport and metabolism Rv3756c
proW Amino acid transport and metabolism Rv3757c
- Carbohydrate transport and metabolism Rv0525
- Carbohydrate transport and metabolism Rv1410c
pmmA Carbohydrate transport and metabolism Rv3257
pgi Carbohydrate transport and metabolism Rv0946c
eccC5 Cell cycle control Rv1783
manB CellWallbiogenesis Rv3264c
thiG Coenzyme transport and metabolism Rv0417
cobO Coenzyme transport and metabolism Rv2849c
folP1 Coenzyme transport and metabolism Rv3608c
- Energy production and conversion Rv0044c
dlaT Energy production and conversion Rv2215
- Energy production and conversion Rv2454c
- Function unknown Rv1836c
lprC Function unknown Rv1275
rskA Function unknown Rv0444c
mce2B Function unknown Rv0590
eccB5 Function unknown Rv1782
eccD5 Function unknown Rv1795
- Function unknown Rv2410c
- Function unknown Rv2446c
- Function unknown Rv3136A
- Function unknown Rv3691
- Function unknown Rv3701c
- Function unknown Rv3703c
- Function unknown Rv3732
- Function unknown Rv0051
- Function unknown Rv2772c
- Function unknown Rv3605c
eccD1 Function unknown Rv3877
- General function prediction only Rv1021
- General function prediction only Rv2004c
eis General function prediction only Rv2416c
mmpL7 General function prediction only Rv2942
secA1 Intracellular trafficking Rv3240c
lipT Lipid transport and metabolism Rv2045c
echA14 Lipid transport and metabolism Rv2486
- Lipid transport and metabolism Rv3814c
- Lipid transport and metabolism Rv3815c
hpt Nucleotide transport and metabolism Rv3624c
pyrH Nucleotide transport and metabolism Rv2883c
- Posttranslational modification Rv0526
pflA Posttranslational modification Rv3138
eccA1 Posttranslational modification Rv3868
deaD Replication Rv1253
mce2A Secondary metabolites biosynthesis Rv0589
pks11 Secondary metabolites biosynthesis Rv1665
ppgK Transcription Rv2702
- Translation Rv1301
hisS Translation Rv2580c

MtbRv

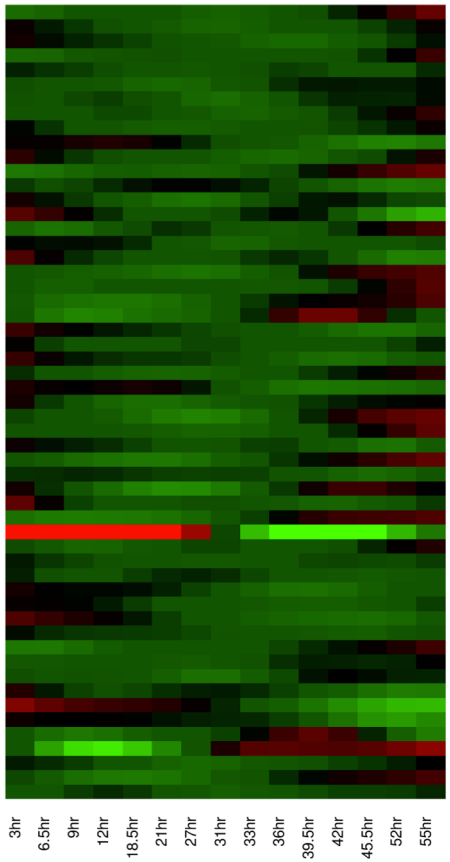

3hr 6.5hr 9hr 12hr 18.5hr 21hr 27hr 31hr 33hr 36hr 39.5hr 42hr 45.5hr 52hr 55hr

- Amino acid transport and metabolism Rv1413
- Amino acid transport and metabolism Rv1769
- Amino acid transport and metabolism Rv2409c
proA Amino acid transport and metabolism Rv2427c
proZ Amino acid transport and metabolism Rv3756c
proW Amino acid transport and metabolism Rv3757c
- Carbohydrate transport and metabolism Rv0525
- Carbohydrate transport and metabolism Rv1410c
pmmA Carbohydrate transport and metabolism Rv3257c
pgi Carbohydrate transport and metabolism Rv0946c
eccC5 Cell cycle control Rv1783
manB CellWallbiogenesis Rv3264c
thiG Coenzyme transport and metabolism Rv0417
cobO Coenzyme transport and metabolism Rv2849c
folP1 Coenzyme transport and metabolism Rv3608c
- Energy production and conversion Rv0044c
dlaT Energy production and conversion Rv2215
- Energy production and conversion Rv2454c
- Function unknown Rv1836c
lprC Function unknown Rv1275
rskA Function unknown Rv0444c
mce2B Function unknown Rv0590
eccB5 Function unknown Rv1782
eccD5 Function unknown Rv1795
- Function unknown Rv2410c
- Function unknown Rv2446c
- Function unknown Rv3136A
- Function unknown Rv3691
- Function unknown Rv3701c
- Function unknown Rv3703c
- Function unknown Rv3732
- Function unknown Rv0051
- Function unknown Rv2772c
- Function unknown Rv3605c
eccD1 Function unknown Rv3877
- General function prediction only Rv1021
- General function prediction only Rv2004c
eis General function prediction only Rv2416c
mmpL7 General function prediction only Rv2942
secA1 Intracellular trafficking Rv3240c
lipT Lipid transport and metabolism Rv2045c
echA14 Lipid transport and metabolism Rv2486
- Lipid transport and metabolism Rv3814c
- Lipid transport and metabolism Rv3815c
hpt Nucleotide transport and metabolism Rv3624c
pyrH Nucleotide transport and metabolism Rv2883c
- Posttranslational modification Rv0526
pflA Posttranslational modification Rv3138
eccA1 Posttranslational modification Rv3868
deaD Replication Rv1253
mce2A Secondary metabolites biosynthesis Rv0589
pks11 Secondary metabolites biosynthesis Rv1665
ppgK Transcription Rv2702
- Translation Rv1301
hisS Translation Rv2580c

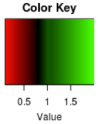

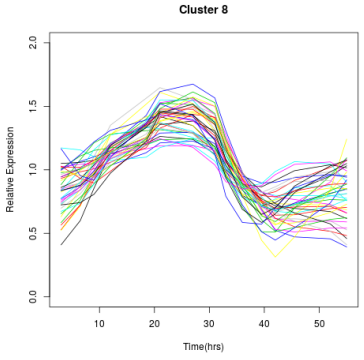

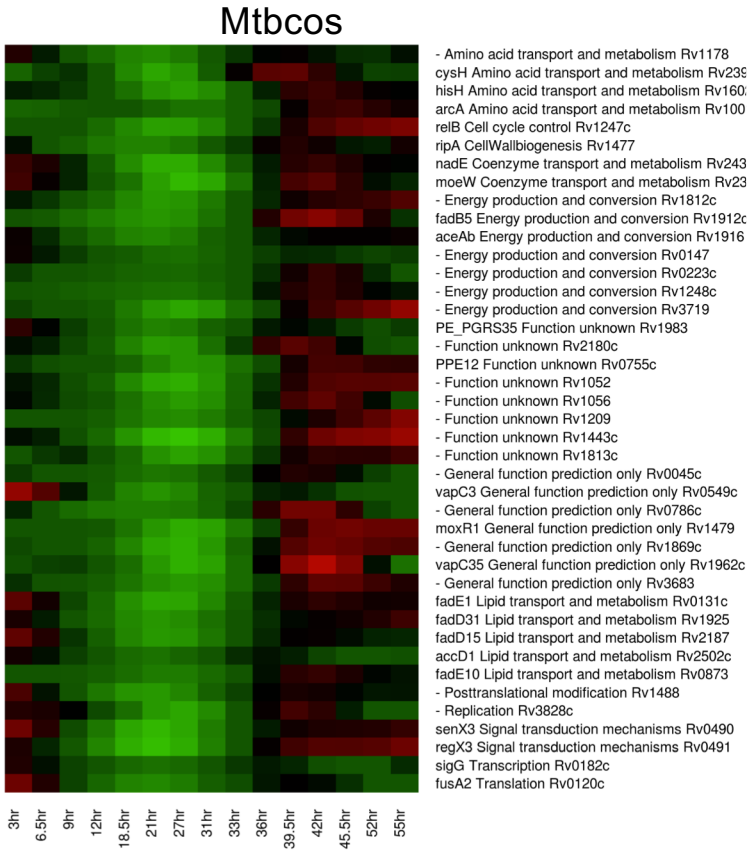

- Amino acid transport and metabolism Rv1178
cysH Amino acid transport and metabolism Rv239
hisH Amino acid transport and metabolism Rv160
arcA Amino acid transport and metabolism Rv100
relB Cell cycle control Rv1247c
ripA CellWallbiogenesis Rv1477
nadE Coenzyme transport and metabolism Rv243
moeW Coenzyme transport and metabolism Rv23
- Energy production and conversion Rv1812c
fadB5 Energy production and conversion Rv1912c
aceAb Energy production and conversion Rv1916
- Energy production and conversion Rv0147
- Energy production and conversion Rv0223c
- Energy production and conversion Rv1248c
- Energy production and conversion Rv3719
PE_PGRS35 Function unknown Rv1983
- Function unknown Rv2180c
PPE12 Function unknown Rv0755c
- Function unknown Rv1052
- Function unknown Rv1056
- Function unknown Rv1209
- Function unknown Rv1443c
- Function unknown Rv1813c
- General function prediction only Rv0045c
vapC3 General function prediction only Rv0549c
- General function prediction only Rv0786c
moxR1 General function prediction only Rv1479
- General function prediction only Rv1869c
vapC35 General function prediction only Rv1962c
- General function prediction only Rv3683
fadE1 Lipid transport and metabolism Rv0131c
fadD31 Lipid transport and metabolism Rv1925
fadD15 Lipid transport and metabolism Rv2187
accD1 Lipid transport and metabolism Rv2502c
fadE10 Lipid transport and metabolism Rv0873
- Posttranslational modification Rv1488
- Replication Rv3828c
senX3 Signal transduction mechanisms Rv0490
regX3 Signal transduction mechanisms Rv0491
sigG Transcription Rv0182c
fusA2 Translation Rv0120c

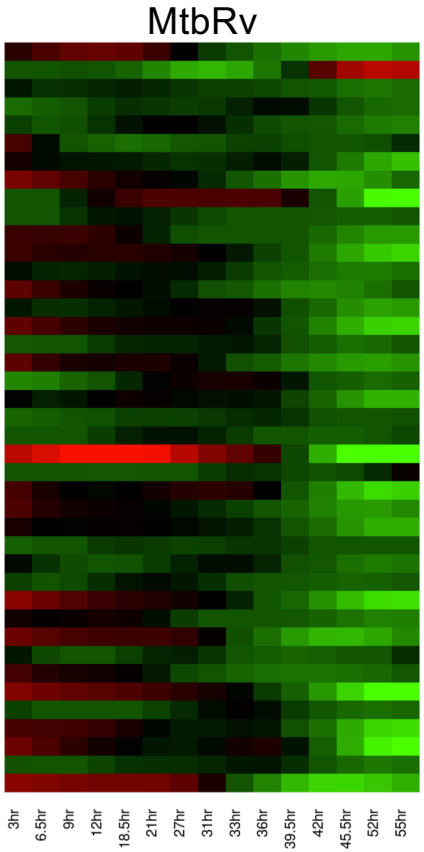

- Amino acid transport and metabolism Rv1178
cysH Amino acid transport and metabolism Rv2392
hisH Amino acid transport and metabolism Rv1602
arcA Amino acid transport and metabolism Rv1001
relB Cell cycle control Rv1247c
ripA CellWallbiogenesis Rv1477
nadE Coenzyme transport and metabolism Rv2438c
moeW Coenzyme transport and metabolism Rv2338c
- Energy production and conversion Rv1812c
fadB5 Energy production and conversion Rv1912c
aceAb Energy production and conversion Rv1916
- Energy production and conversion Rv0147
- Energy production and conversion Rv0223c
- Energy production and conversion Rv1248c
- Energy production and conversion Rv3719
PE_PGRS35 Function unknown Rv1983
- Function unknown Rv2180c
PPE12 Function unknown Rv0755c
- Function unknown Rv1052
- Function unknown Rv1056
- Function unknown Rv1209
- Function unknown Rv1443c
- Function unknown Rv1813c
- General function prediction only Rv0045c
vapC3 General function prediction only Rv0549c
- General function prediction only Rv0786c
moxR1 General function prediction only Rv1479
- General function prediction only Rv1869c
vapC35 General function prediction only Rv1962c
- General function prediction only Rv3683
fadE1 Lipid transport and metabolism Rv0131c
fadD31 Lipid transport and metabolism Rv1925
fadD15 Lipid transport and metabolism Rv2187
accD1 Lipid transport and metabolism Rv2502c
fadE10 Lipid transport and metabolism Rv0873
- Posttranslational modification Rv1488
- Replication Rv3828c
senX3 Signal transduction mechanisms Rv0490
regX3 Signal transduction mechanisms Rv0491
sigG Transcription Rv0182c
fusA2 Translation Rv0120c

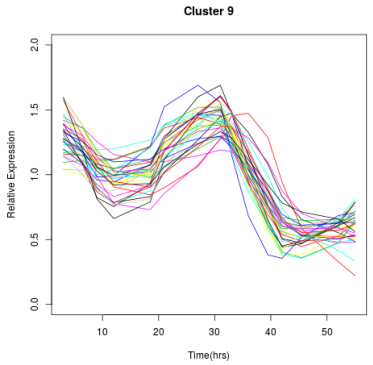

Mtbcos

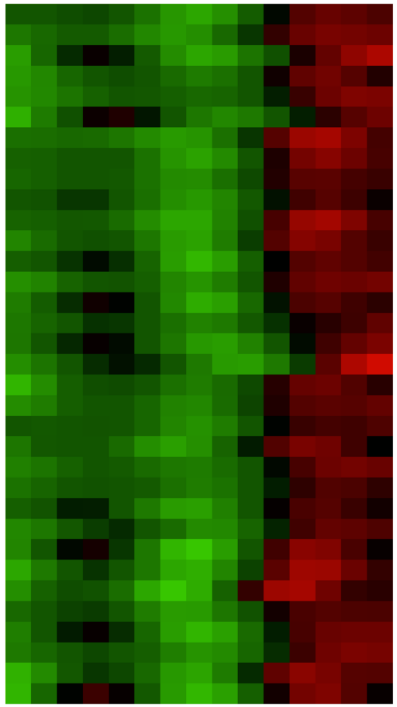

3hr 6.5hr 9hr 12hr 18.5hr 21hr 27hr 31hr 33hr 36hr 39.5hr 42hr 45.5hr 52hr 55hr

fba Carbohydrate transport and metabolism Rv0363c
murA CellWallbiogenesis Rv1315
mscL CellWallbiogenesis Rv0985c
dfrA Coenzyme transport and metabolism Rv2763c
- Function unknown Rv0314c
rpfB Function unknown Rv1009
- Function unknown Rv0309
- Function unknown Rv0190
- Function unknown Rv0192A
- Function unknown Rv0323c
- Function unknown Rv0730
- Function unknown Rv1314c
- Function unknown Rv2018
PPE59 Function unknown Rv3429
- Function unknown Rv3686c
- Function unknown Rv3716c
- Function unknown Rv0531
- Function unknown Rv0609A
obg General function prediction only Rv2440c
phoY1 Inorganic ion transport and metabolism Rv3301c
modC Inorganic ion transport and metabolism Rv1859
- Intracellular trafficking Rv1944c
- Lipid transport and metabolism Rv2766c
- Lipid transport and metabolism Rv0769
- Lipid transport and metabolism Rv1245c
trxB2 Posttranslational modification Rv3913
ssb Replication Rv0054
- Replication Rv2309c
mazF5 Signal transduction mechanisms Rv1942c
- Transcription Rv0238
sigA Transcription Rv2703
- Transcription Rv2840c
rplY Translation Rv1015c
rpmA Translation Rv2441c

MtbRv

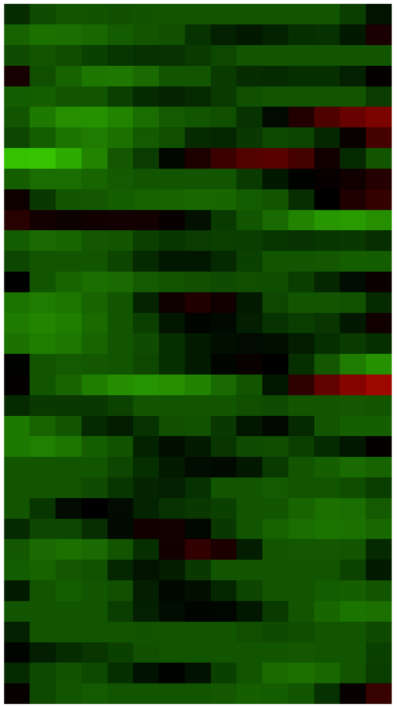

3hr 6.5hr 9hr 12hr 18.5hr 21hr 27hr 31hr 33hr 36hr 39.5hr 42hr 45.5hr 52hr 55hr

fba Carbohydrate transport and metabolism Rv0363c
murA CellWallbiogenesis Rv1315
mscL CellWallbiogenesis Rv0985c
dfrA Coenzyme transport and metabolism Rv2763c
- Function unknown Rv0314c
rpfB Function unknown Rv1009
- Function unknown Rv0309
- Function unknown Rv0190
- Function unknown Rv0192A
- Function unknown Rv0323c
- Function unknown Rv0730
- Function unknown Rv1314c
- Function unknown Rv2018
PPE59 Function unknown Rv3429
- Function unknown Rv3686c
- Function unknown Rv3716c
- Function unknown Rv0531
- Function unknown Rv0609A
obg General function prediction only Rv2440c
phoY1 Inorganic ion transport and metabolism Rv3301c
modC Inorganic ion transport and metabolism Rv1859
- Intracellular trafficking Rv1944c
- Lipid transport and metabolism Rv2766c
- Lipid transport and metabolism Rv0769
- Lipid transport and metabolism Rv1245c
trxB2 Posttranslational modification Rv3913
ssb Replication Rv0054
- Replication Rv2309c
mazF5 Signal transduction mechanisms Rv1942c
- Transcription Rv0238
sigA Transcription Rv2703
- Transcription Rv2840c
rplY Translation Rv1015c
rpmA Translation Rv2441c

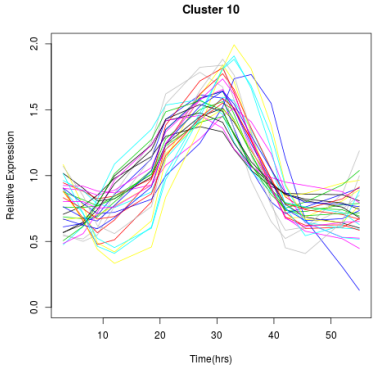

Mtbcos

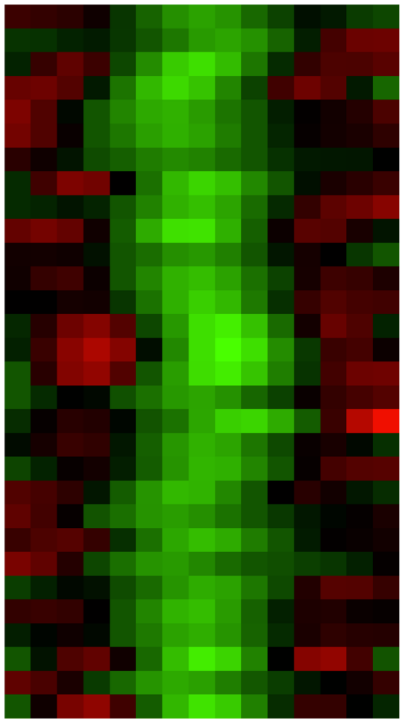

wag31 Cell cycle control Rv2145c
mmaA1 CellWallbiogenesis Rv0645c
panB Coenzyme transport and metabolism Rv22
- Energy production and conversion Rv0763c
acg Energy production and conversion Rv2032
kstD Energy production and conversion Rv3537
- Function unknown Rv1100
PPE19 Function unknown Rv1361c
fxsA Function unknown Rv2053c
- Function unknown Rv2172c
aprB Function unknown Rv2395B
- Function unknown Rv2639c
- Function unknown Rv3848
- Function unknown Rv2645
- Function unknown Rv2699c
- Function unknown Rv3603c
- General function prediction only Rv0060
- General function prediction only Rv1986
- Inorganic ion transport and metabolism Rv3161
secE1 Intracellular trafficking Rv0638
fadE6 Lipid transport and metabolism Rv0271c
- Lipid transport and metabolism Rv2182c
ispD Lipid transport and metabolism Rv3582c
- Secondary metabolites biosynthesis Rv2675c
- Secondary metabolites biosynthesis Rv0145
- Secondary metabolites biosynthesis Rv0146
garA Signal transduction mechanisms Rv1827
mazE9 Signal transduction mechanisms Rv2801
rnc Transcription Rv2925c
rpoB Transcription Rv0667

3hr 6.5hr 9hr 12hr 18.5hr 21hr 27hr 31hr 33hr 36hr 39.5hr 42hr 45.5hr 52hr 55hr

MtbRv

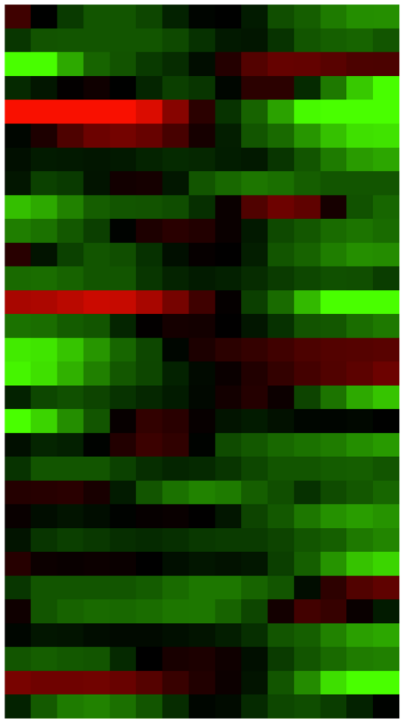

wag31 Cell cycle control Rv2145c
mmaA1 CellWallbiogenesis Rv0645c
panB Coenzyme transport and metabolism Rv2225
- Energy production and conversion Rv0763c
acg Energy production and conversion Rv2032
kstD Energy production and conversion Rv3537
- Function unknown Rv1100
PPE19 Function unknown Rv1361c
fxsA Function unknown Rv2053c
- Function unknown Rv2172c
aprB Function unknown Rv2395B
- Function unknown Rv2639c
- Function unknown Rv3848
- Function unknown Rv2645
- Function unknown Rv2699c
- Function unknown Rv3603c
- General function prediction only Rv0060
- General function prediction only Rv1986
- Inorganic ion transport and metabolism Rv3161c
secE1 Intracellular trafficking Rv0638
fadE6 Lipid transport and metabolism Rv0271c
- Lipid transport and metabolism Rv2182c
ispD Lipid transport and metabolism Rv3582c
- Secondary metabolites biosynthesis Rv2675c
- Secondary metabolites biosynthesis Rv0145
- Secondary metabolites biosynthesis Rv0146
garA Signal transduction mechanisms Rv1827
mazE9 Signal transduction mechanisms Rv2801A
rnc Transcription Rv2925c
rpoB Transcription Rv0667

3hr 6.5hr 9hr 12hr 18.5hr 21hr 27hr 31hr 33hr 36hr 39.5hr 42hr 45.5hr 52hr 55hr

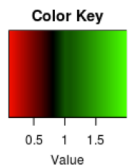

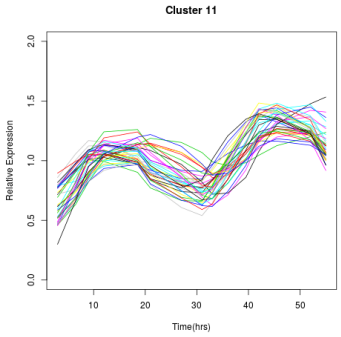

Mtbcos

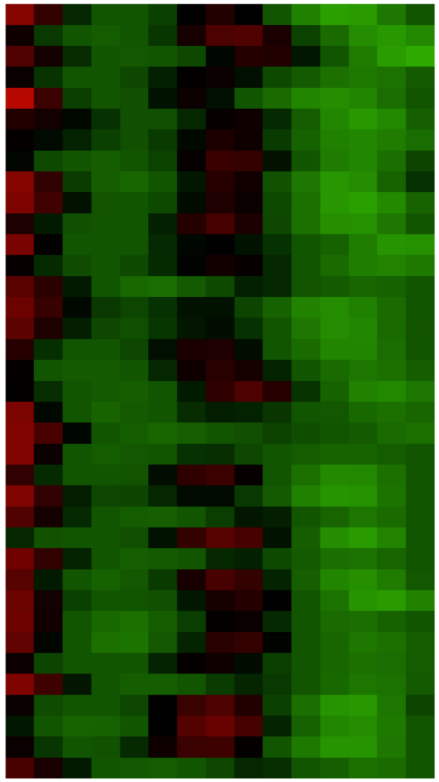

gabP Amino acid transport and metabolism Rv0522
aroE Amino acid transport and metabolism Rv2552c
hisF Amino acid transport and metabolism Rv1605
- Cell cycle control Rv0530
dacB1 CellWallbiogenesis Rv3330
murC CellWallbiogenesis Rv2152c
thiE Coenzyme transport and metabolism Rv0414c
idsA2 Coenzyme transport and metabolism Rv2173
- Energy production and conversion Rv2776c
narX Energy production and conversion Rv1736c
leuB Energy production and conversion Rv2995c
- Energy production and conversion Rv0458
- Energy production and conversion Rv1257c
- Function unknown Rv3626c
- Function unknown Rv0398c
- Function unknown Rv1486c
- Function unknown Rv0080
- Function unknown Rv1510
whiA Function unknown Rv1423
PE_PGRS31 Function unknown Rv1768
- Function unknown Rv0307c
- General function prediction only Rv1220c
- General function prediction only Rv1639c
- General function prediction only Rv3312c
- General function prediction only Rv0245
- General function prediction only Rv3422c
- General function prediction only Rv3542c
- General function prediction only Rv3813c
recX General function prediction only Rv2736c
- Inorganic ion transport and metabolism Rv2325c
- Inorganic ion transport and metabolism Rv2326c
echA4 Lipid transport and metabolism Rv0673
- Lipid transport and metabolism Rv1627c
fadE16 Lipid transport and metabolism Rv1679
- Posttranslational modification Rv0528
mfd Replication Rv1020
erm(37) Translation Rv1988

MtbRv

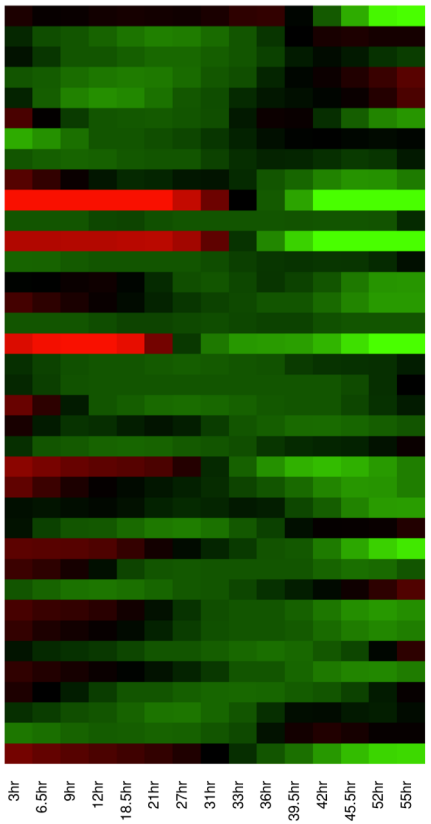

gabP Amino acid transport and metabolism Rv0522
aroE Amino acid transport and metabolism Rv2552c
hisF Amino acid transport and metabolism Rv1605
- Cell cycle control Rv0530
dacB1 CellWallbiogenesis Rv3330
murC CellWallbiogenesis Rv2152c
thiE Coenzyme transport and metabolism Rv0414c
idsA2 Coenzyme transport and metabolism Rv2173
- Energy production and conversion Rv2776c
narX Energy production and conversion Rv1736c
leuB Energy production and conversion Rv2995c
- Energy production and conversion Rv0458
- Energy production and conversion Rv1257c
- Function unknown Rv3626c
- Function unknown Rv0398c
- Function unknown Rv1486c
- Function unknown Rv0080
- Function unknown Rv1510
whiA Function unknown Rv1423
PE_PGRS31 Function unknown Rv1768
- Function unknown Rv0307c
- General function prediction only Rv1220c
- General function prediction only Rv1639c
- General function prediction only Rv3312c
- General function prediction only Rv0245
- General function prediction only Rv3422c
- General function prediction only Rv3542c
- General function prediction only Rv3813c
recX General function prediction only Rv2736c
- Inorganic ion transport and metabolism Rv2325c
- Inorganic ion transport and metabolism Rv2326c
echA4 Lipid transport and metabolism Rv0673
- Lipid transport and metabolism Rv1627c
fadE16 Lipid transport and metabolism Rv1679
- Posttranslational modification Rv0528
mfd Replication Rv1020
erm(37) Translation Rv1988

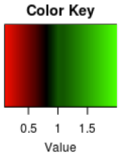

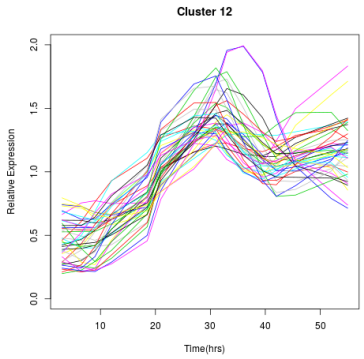

Mtbcos

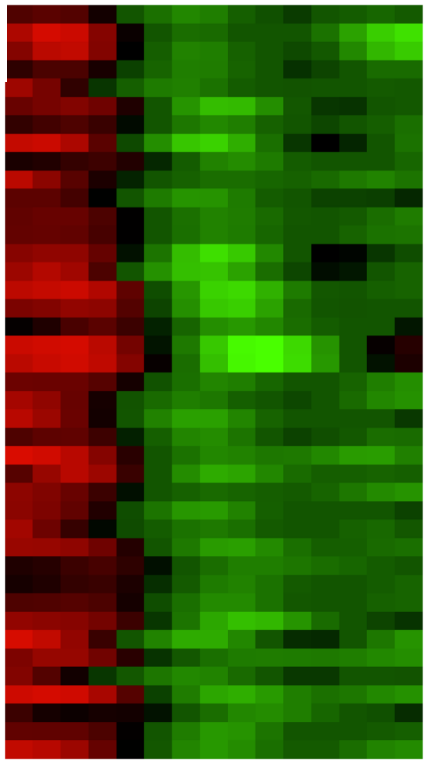

3hr 6.5hr 9hr 12hr 18.5hr 21hr 27hr 31hr 33hr 36hr 39.5hr 42hr 45.5hr 52hr 55hr

gcvB Amino acid transport and metabolism Rv1832
cysK2 Amino acid transport and metabolism Rv0848
- Carbohydrate transport and metabolism Rv0849
murD CellWallbiogenesis Rv2155c
- CellWallbiogenesis Rv2165c
- Energy production and conversion Rv0940c
sthA Energy production and conversion Rv2713
- Energy production and conversion Rv3230c
aldA Energy production and conversion Rv0768
fgd2 Energy production and conversion Rv0132c
- Function unknown Rv3847
- Function unknown Rv2015c
- Function unknown Rv2302
- Function unknown Rv3182
cut5a Function unknown Rv3724A
- Function unknown Rv1588c
rpfC Function unknown Rv1884c
- Function unknown Rv2295
- Function unknown Rv2656c
- Function unknown Rv2714
hbhA Function unknown Rv0475
- Function unknown Rv1861
- General function prediction only Rv2867c
- General function prediction only Rv1833c
- General function prediction only Rv2650c
- Inorganic ion transport and metabolism Rv2025c
katG Inorganic ion transport and metabolism Rv1908c
fadE28 Lipid transport and metabolism Rv3544c
- Lipid transport and metabolism Rv3551
scoA Lipid transport and metabolism Rv2504c
ispF Lipid transport and metabolism Rv3581c
thyA Nucleotide transport and metabolism Rv2764c
pepD Posttranslational modification Rv0983
mpt53 Posttranslational modification Rv2878c
hupB Replication Rv2986c
- Secondary metabolites biosynthesis Rv0846c
phoH2 Signal transduction mechanisms Rv1095
arsC Signal transduction mechanisms Rv2643
- Signal transduction mechanisms Rv2242
- Transcription Rv1765c
- Translation Rv0088

MtbRv

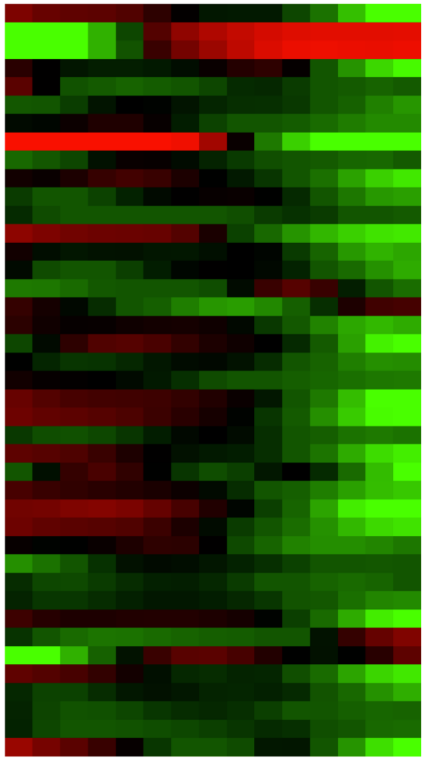

3hr 6.5hr 9hr 12hr 18.5hr 21hr 27hr 31hr 33hr 36hr 39.5hr 42hr 45.5hr 52hr 55hr

gcvB Amino acid transport and metabolism Rv1832
cysK2 Amino acid transport and metabolism Rv0848
- Carbohydrate transport and metabolism Rv0849
murD CellWallbiogenesis Rv2155c
- CellWallbiogenesis Rv2165c
- Energy production and conversion Rv0940c
sthA Energy production and conversion Rv2713
- Energy production and conversion Rv3230c
aldA Energy production and conversion Rv0768
fgd2 Energy production and conversion Rv0132c
- Function unknown Rv3847
- Function unknown Rv2015c
- Function unknown Rv2302
- Function unknown Rv3182
cut5a Function unknown Rv3724A
- Function unknown Rv1588c
rpfC Function unknown Rv1884c
- Function unknown Rv2295
- Function unknown Rv2656c
- Function unknown Rv2714
hbhA Function unknown Rv0475
- Function unknown Rv1861
- General function prediction only Rv2867c
- General function prediction only Rv1833c
- General function prediction only Rv2650c
- Inorganic ion transport and metabolism Rv2025c
katG Inorganic ion transport and metabolism Rv1908c
fadE28 Lipid transport and metabolism Rv3544c
- Lipid transport and metabolism Rv3551
scoA Lipid transport and metabolism Rv2504c
ispF Lipid transport and metabolism Rv3581c
thyA Nucleotide transport and metabolism Rv2764c
pepD Posttranslational modification Rv0983
mpt53 Posttranslational modification Rv2878c
hupB Replication Rv2986c
- Secondary metabolites biosynthesis Rv0846c
phoH2 Signal transduction mechanisms Rv1095
arsC Signal transduction mechanisms Rv2643
- Signal transduction mechanisms Rv2242
- Transcription Rv1765c
- Translation Rv0088

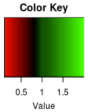

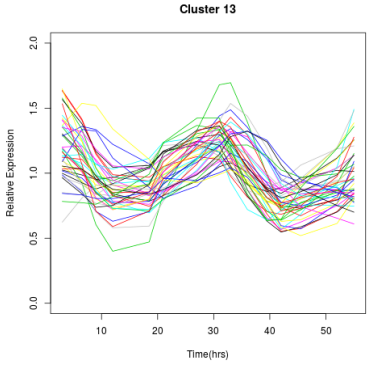

Mtbcos

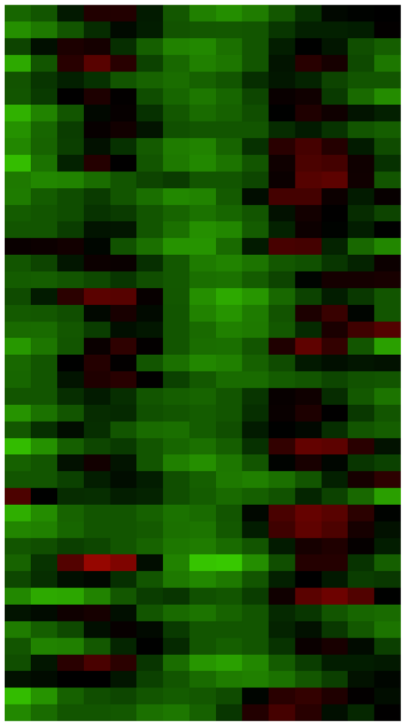

3hr 6.5hr 9hr 12hr 18.5hr 21hr 27hr 31hr 33hr 36hr 39.5hr 42hr 45.5hr 52hr 55hr

sugI Carbohydrate transport and metabolism Rv3331
vapB5 Cell cycle control Rv0626
mpt83 CellWallbiogenesis Rv2873
panD Coenzyme transport and metabolism Rv3601c
glcB Energy production and conversion Rv1837c
gabD2 Energy production and conversion Rv1731
mshB Function unknown Rv1170
mihF Function unknown Rv1388
dedA Function unknown Rv2637
- Function unknown Rv2734
- Function unknown Rv1951c
mazE5 Function unknown Rv1943c
- Function unknown Rv0611c
- Function unknown Rv2513
PE_PGRS60 Function unknown Rv3652
- Function unknown Rv1171
- Function unknown Rv1249c
mgtC Function unknown Rv1811
- Function unknown Rv1875
- Function unknown Rv2219A
- Function unknown Rv2081c
- General function prediction only Rv2715
- General function prediction only Rv3034c
- General function prediction only Rv2296
atsD Inorganic ion transport and metabolism Rv0663
sirA Inorganic ion transport and metabolism Rv2391
fadE4 Lipid transport and metabolism Rv0231
fadD26 Lipid transport and metabolism Rv2930
fadA6 Lipid transport and metabolism Rv3556c
echA19 Lipid transport and metabolism Rv3516
clpP1 Posttranslational modification Rv2461c
groEL1 Posttranslational modification Rv3417c
pepA Posttranslational modification Rv0125
dnaK Posttranslational modification Rv0350
- Replication Rv0741
yrbE4B Secondary metabolites biosynthesis Rv3500c
mazF9 Signal transduction mechanisms Rv2801c
- Transcription Rv0880
- Transcription Rv2669
- Transcription Rv0465c
- Transcription Rv3160c
pth Translation Rv1014c
- Translation Rv2704

MtbRv

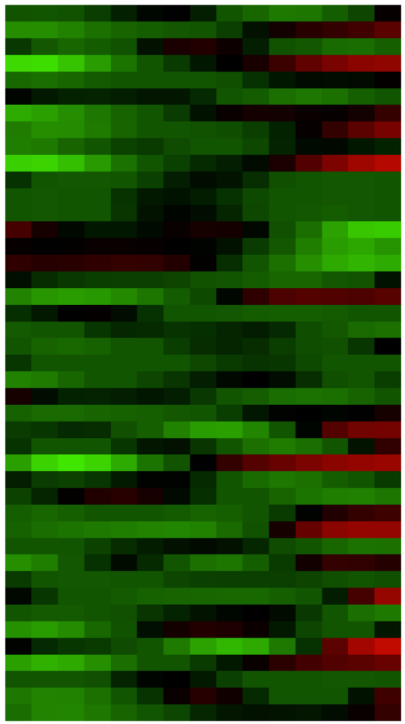

3hr 6.5hr 9hr 12hr 18.5hr 21hr 27hr 31hr 33hr 36hr 39.5hr 42hr 45.5hr 52hr 55hr

sugI Carbohydrate transport and metabolism Rv3331
vapB5 Cell cycle control Rv0626
mpt83 CellWallbiogenesis Rv2873
panD Coenzyme transport and metabolism Rv3601c
glcB Energy production and conversion Rv1837c
gabD2 Energy production and conversion Rv1731
mshB Function unknown Rv1170
mihF Function unknown Rv1388
dedA Function unknown Rv2637
- Function unknown Rv2734
- Function unknown Rv1951c
mazE5 Function unknown Rv1943c
- Function unknown Rv0611c
- Function unknown Rv2513
PE_PGRS60 Function unknown Rv3652
- Function unknown Rv1171
- Function unknown Rv1249c
mgtC Function unknown Rv1811
- Function unknown Rv1875
- Function unknown Rv2219A
- Function unknown Rv2081c
- General function prediction only Rv2715
- General function prediction only Rv3034c
- General function prediction only Rv2296
atsD Inorganic ion transport and metabolism Rv0663
sirA Inorganic ion transport and metabolism Rv2391
fadE4 Lipid transport and metabolism Rv0231
fadD26 Lipid transport and metabolism Rv2930
fadA6 Lipid transport and metabolism Rv3556c
echA19 Lipid transport and metabolism Rv3516
clpP1 Posttranslational modification Rv2461c
groEL1 Posttranslational modification Rv3417c
pepA Posttranslational modification Rv0125
dnaK Posttranslational modification Rv0350
- Replication Rv0741
yrbE4B Secondary metabolites biosynthesis Rv3500c
mazF9 Signal transduction mechanisms Rv2801c
- Transcription Rv0880
- Transcription Rv2669
- Transcription Rv0465c
- Transcription Rv3160c
pth Translation Rv1014c
- Translation Rv2704

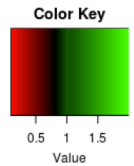

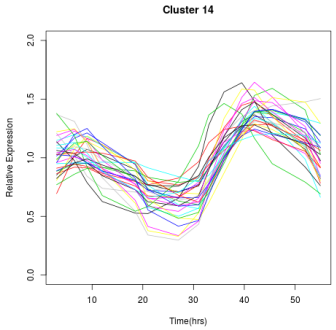

Mtbcos

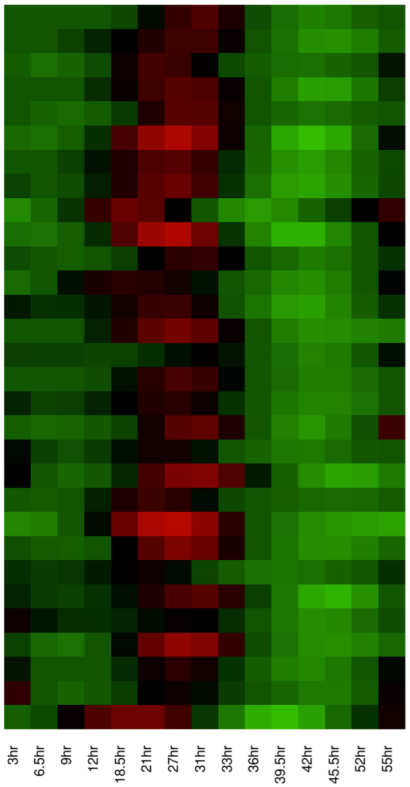

3hr 6.5hr 9hr 12hr 18.5hr 21hr 27hr 31hr 33hr 36hr 39.5hr 42hr 45.5hr 52hr 55hr

mutT1 Carbohydrate transport and metabolism Rv2985
- Carbohydrate transport and metabolism Rv2135c
mgtA CellWallbiogenesis Rv0557
- CellWallbiogenesis Rv3786c
pncB1 Coenzyme transport and metabolism Rv1330c
bioA Coenzyme transport and metabolism Rv1568
cobH Coenzyme transport and metabolism Rv2065
ribD Coenzyme transport and metabolism Rv2671
- Function unknown Rv2076c
- Function unknown Rv1590
- Function unknown Rv0910
- Function unknown Rv0965c
- Function unknown Rv1117
- Function unknown Rv1382
vapB38 Function unknown Rv2493
- Function unknown Rv2844
- General function prediction only Rv0406c
- General function prediction only Rv0421c
mqo General function prediction only Rv2852c
pepR General function prediction only Rv2782c
- General function prediction only Rv3586
engA General function prediction only Rv1713
fecB Inorganic ion transport and metabolism Rv3044
- Lipid transport and metabolism Rv2073c
- Lipid transport and metabolism Rv0228
htrA Posttranslational modification Rv1223
lprN Secondary metabolites biosynthesis Rv3495c
- Transcription Rv0133
mce1R Transcription Rv0165c
ksgA Translation Rv1010

MtbRv

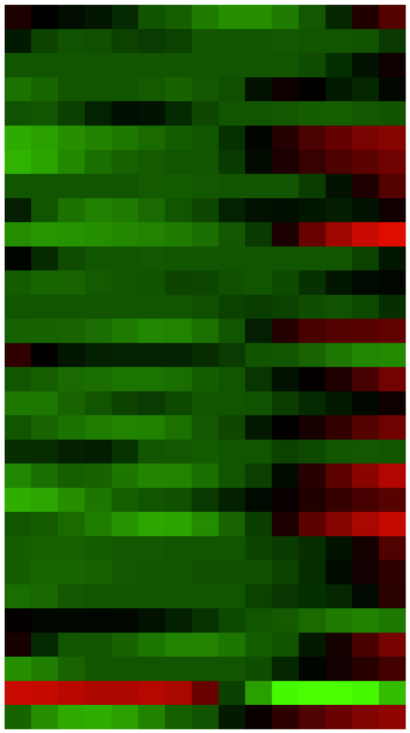

3hr 6.5hr 9hr 12hr 18.5hr 21hr 27hr 31hr 33hr 36hr 39.5hr 42hr 45.5hr 52hr 55hr

mutT1 Carbohydrate transport and metabolism Rv2985
- Carbohydrate transport and metabolism Rv2135c
mgtA CellWallbiogenesis Rv0557
- CellWallbiogenesis Rv3786c
pncB1 Coenzyme transport and metabolism Rv1330c
bioA Coenzyme transport and metabolism Rv1568
cobH Coenzyme transport and metabolism Rv2065
ribD Coenzyme transport and metabolism Rv2671
- Function unknown Rv2076c
- Function unknown Rv1590
- Function unknown Rv0910
- Function unknown Rv0965c
- Function unknown Rv1117
- Function unknown Rv1382
vapB38 Function unknown Rv2493
- Function unknown Rv2844
- General function prediction only Rv0406c
- General function prediction only Rv0421c
mqo General function prediction only Rv2852c
pepR General function prediction only Rv2782c
- General function prediction only Rv3586
engA General function prediction only Rv1713
fecB Inorganic ion transport and metabolism Rv3044
- Lipid transport and metabolism Rv2073c
- Lipid transport and metabolism Rv0228
htrA Posttranslational modification Rv1223
lprN Secondary metabolites biosynthesis Rv3495c
- Transcription Rv0133
mce1R Transcription Rv0165c
ksgA Translation Rv1010

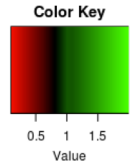

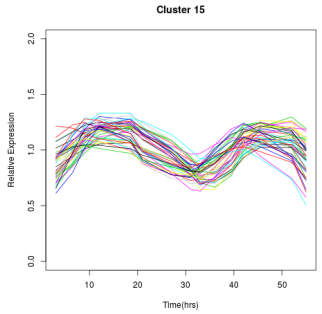

Mtbcos

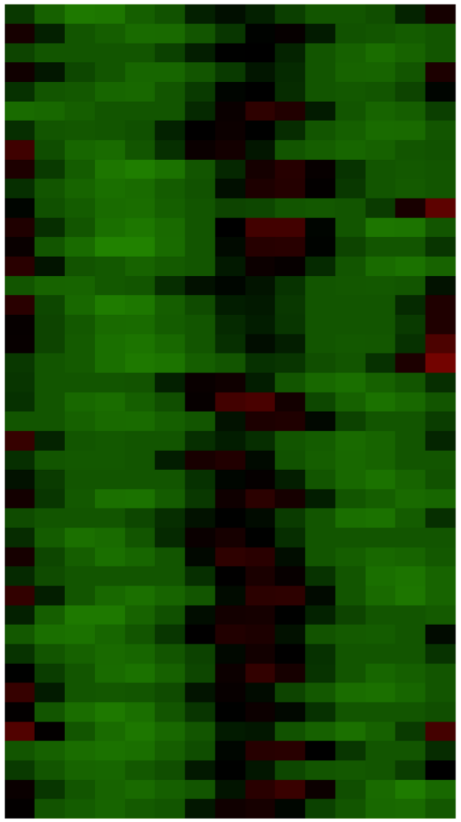

3hr 6.5hr 9hr 12hr 18.5hr 21hr 27hr 31hr 33hr 36hr 39.5hr 42hr 45.5hr 52hr 55hr

proV Amino acid transport and metabolism Rv3758c
trpD Amino acid transport and metabolism Rv2192c
asd Amino acid transport and metabolism Rv3708c
impA Carbohydrate transport and metabolism Rv1604
mrp Cell cycle control Rv1229c
ftsQ CellWallbiogenesis Rv2151c
glmS CellWallbiogenesis Rv3436c
cobB Coenzyme transport and metabolism Rv2848c
folE Coenzyme transport and metabolism Rv3609c
lipD Defense mechanisms Rv1923
- Defense mechanisms Rv1922
narJ Energy production and conversion Rv1163
- Energy production and conversion Rv2251
narH Energy production and conversion Rv1162
- Function unknown Rv1126c
- Function unknown Rv0460
- Function unknown Rv0204c
vapC43 Function unknown Rv2872
- Function unknown Rv3217c
- Function unknown Rv0513
- Function unknown Rv3256c
- General function prediction only Rv0906
mmpL2 General function prediction only Rv0507
- General function prediction only Rv1215c
- General function prediction only Rv0181c
cysA1 Inorganic ion transport and metabolism Rv2397c
viuB Inorganic ion transport and metabolism Rv2895c
fadA3 Lipid transport and metabolism Rv1074c
plsC Lipid transport and metabolism Rv2483c
echA5 Lipid transport and metabolism Rv0675
fadE9 Lipid transport and metabolism Rv0752c
guaB1 Nucleotide transport and metabolism Rv1843c
- Posttranslational modification Rv1456c
uvrD1 Replication Rv0949
polA Replication Rv1629
- Signal transduction mechanisms Rv0386
pafB Transcription Rv2096c
- Transcription Rv2250A
mshC Translation Rv2130c
gatB Translation Rv3009c
rimJ Translation Rv0995
rne Translation Rv2444c

MtbRv

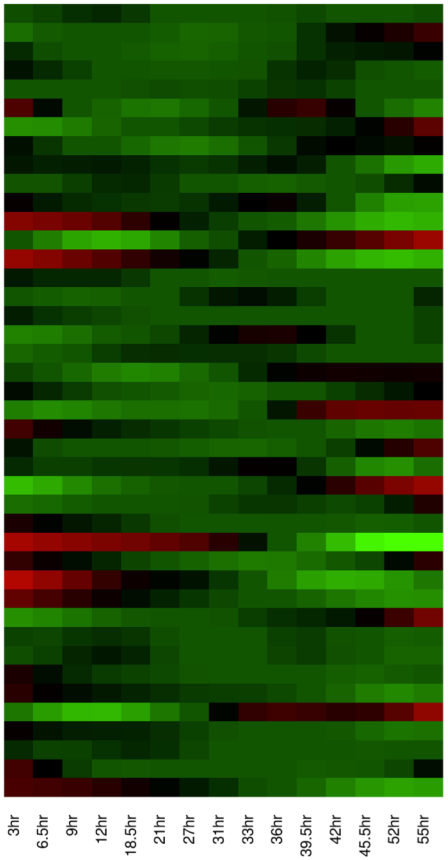

3hr 6.5hr 9hr 12hr 18.5hr 21hr 27hr 31hr 33hr 36hr 39.5hr 42hr 45.5hr 52hr 55hr

proV Amino acid transport and metabolism Rv3758c
trpD Amino acid transport and metabolism Rv2192c
asd Amino acid transport and metabolism Rv3708c
impA Carbohydrate transport and metabolism Rv1604
mrp Cell cycle control Rv1229c
ftsQ CellWallbiogenesis Rv2151c
glmS CellWallbiogenesis Rv3436c
cobB Coenzyme transport and metabolism Rv2848c
folE Coenzyme transport and metabolism Rv3609c
lipD Defense mechanisms Rv1923
- Defense mechanisms Rv1922
narJ Energy production and conversion Rv1163
- Energy production and conversion Rv2251
narH Energy production and conversion Rv1162
- Function unknown Rv1126c
- Function unknown Rv0460
- Function unknown Rv0204c
vapC43 Function unknown Rv2872
- Function unknown Rv3217c
- Function unknown Rv0513
- Function unknown Rv3256c
- General function prediction only Rv0906
mmpL2 General function prediction only Rv0507
- General function prediction only Rv1215c
- General function prediction only Rv0181c
cysA1 Inorganic ion transport and metabolism Rv2397c
viuB Inorganic ion transport and metabolism Rv2895c
fadA3 Lipid transport and metabolism Rv1074c
plsC Lipid transport and metabolism Rv2483c
echA5 Lipid transport and metabolism Rv0675
fadE9 Lipid transport and metabolism Rv0752c
guaB1 Nucleotide transport and metabolism Rv1843c
- Posttranslational modification Rv1456c
uvrD1 Replication Rv0949
polA Replication Rv1629
- Signal transduction mechanisms Rv0386
pafB Transcription Rv2096c
- Transcription Rv2250A
mshC Translation Rv2130c
gatB Translation Rv3009c
rimJ Translation Rv0995
rne Translation Rv2444c

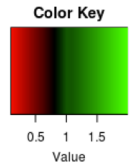

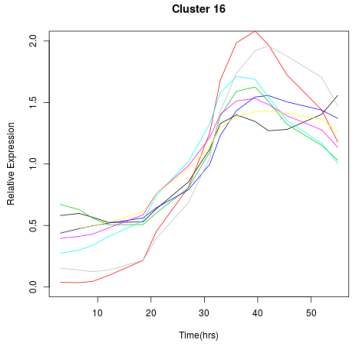
Cluster 16
Relative Expression
0.0
0.5
1.0
1.5
2.0
10
20
30
40
50
Time(hrs)

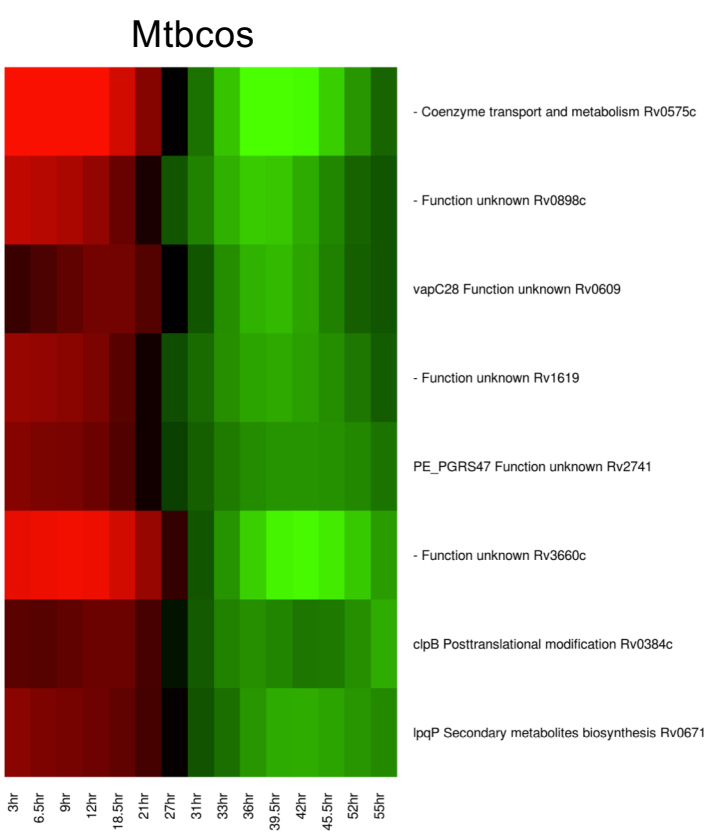
Mtbcos
- Coenzyme transport and metabolism Rv0575c
- Function unknown Rv0898c
vapC28 Function unknown Rv0609
- Function unknown Rv1619
PE_PGRS47 Function unknown Rv2741
- Function unknown Rv3660c
clpB Posttranslational modification Rv0384c
lpqP Secondary metabolites biosynthesis Rv0671
3hr
6.5hr
9hr
12hr
18.5hr
21hr
27hr
31hr
33hr
36hr
39.5hr
42hr
45.5hr
52hr
55hr

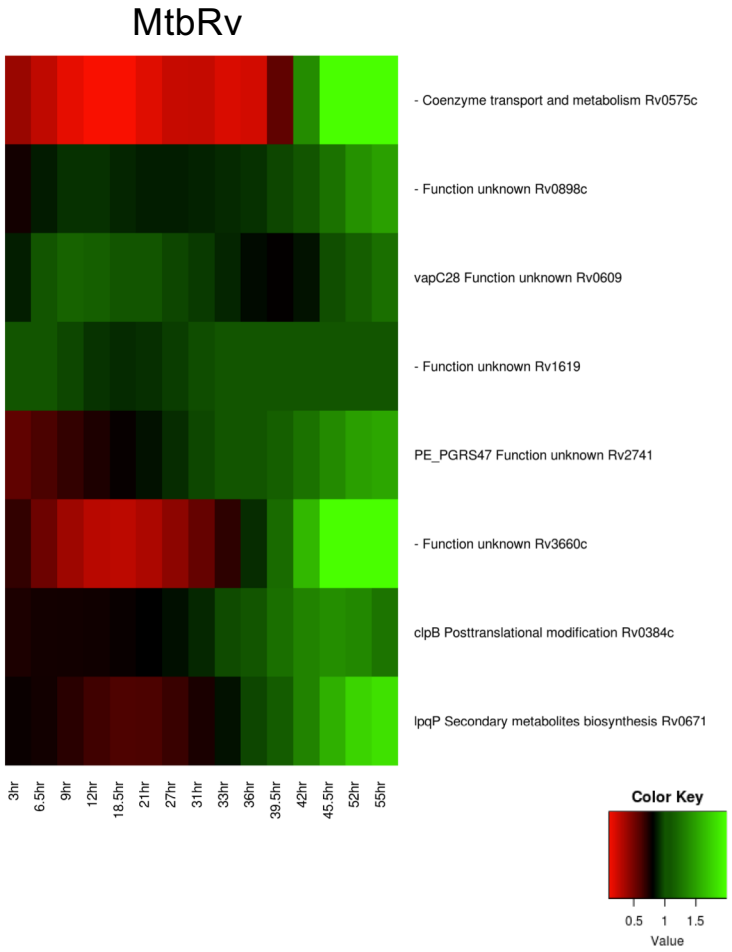
MtbRv
- Coenzyme transport and metabolism Rv0575c
- Function unknown Rv0898c
vapC28 Function unknown Rv0609
- Function unknown Rv1619
PE_PGRS47 Function unknown Rv2741
- Function unknown Rv3660c
clpB Posttranslational modification Rv0384c
lpqP Secondary metabolites biosynthesis Rv0671
3hr
6.5hr
9hr
12hr
18.5hr
21hr
27hr
31hr
33hr
36hr
39.5hr
42hr
45.5hr
52hr
55hr
Color Key
0.5
1
1.5
Value

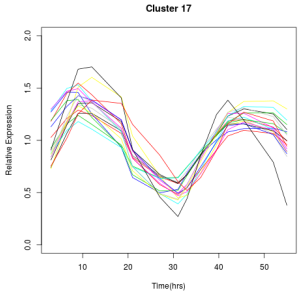

Mtbcos

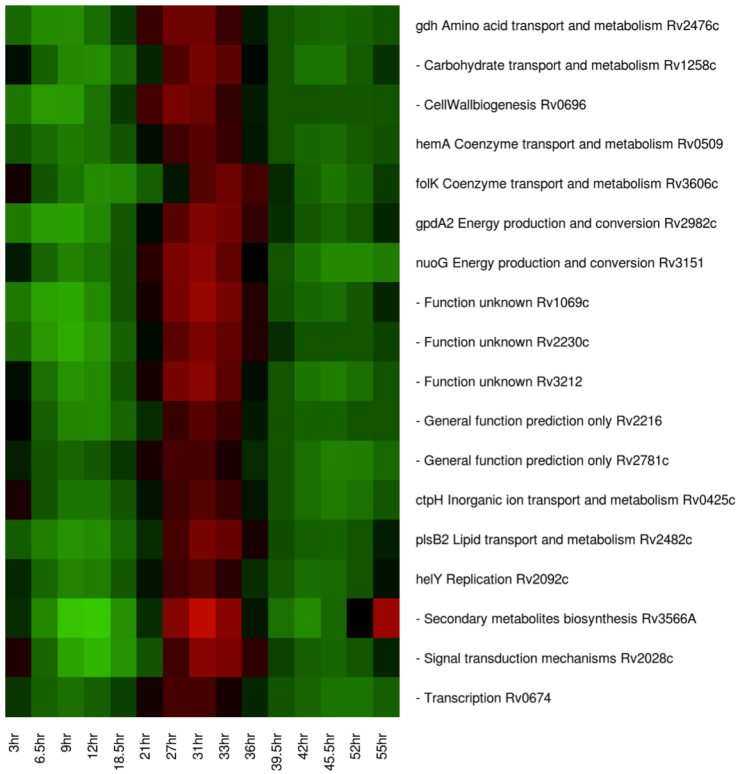

MtbRv

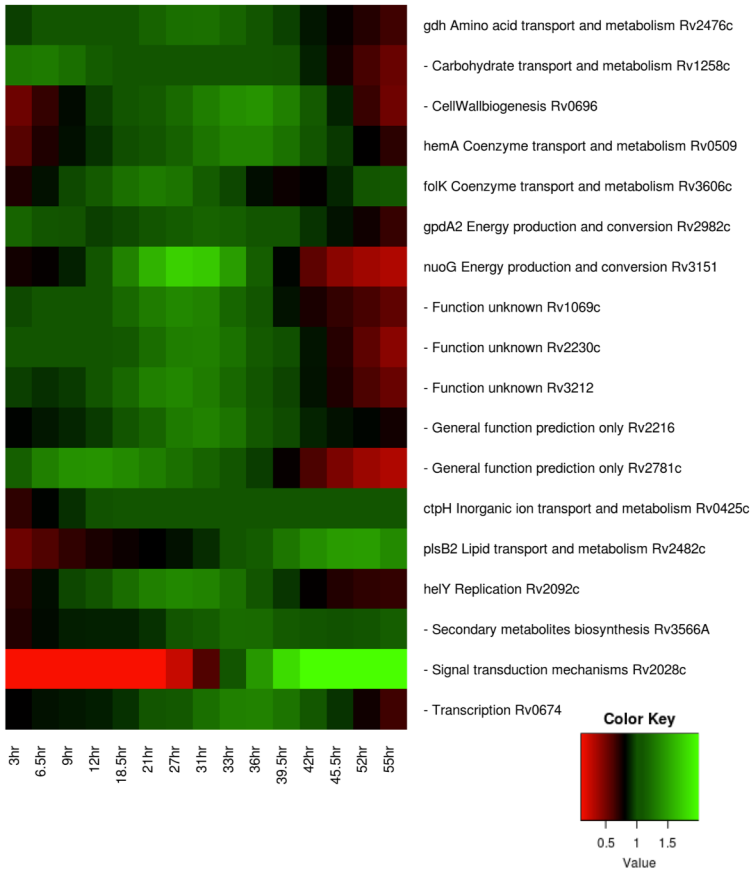

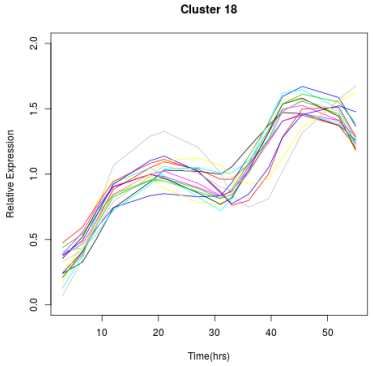
Cluster 18
Relative Expression
0.0
0.5
1.0
1.5
2.0
10
20
30
40
50
Time(hrs)

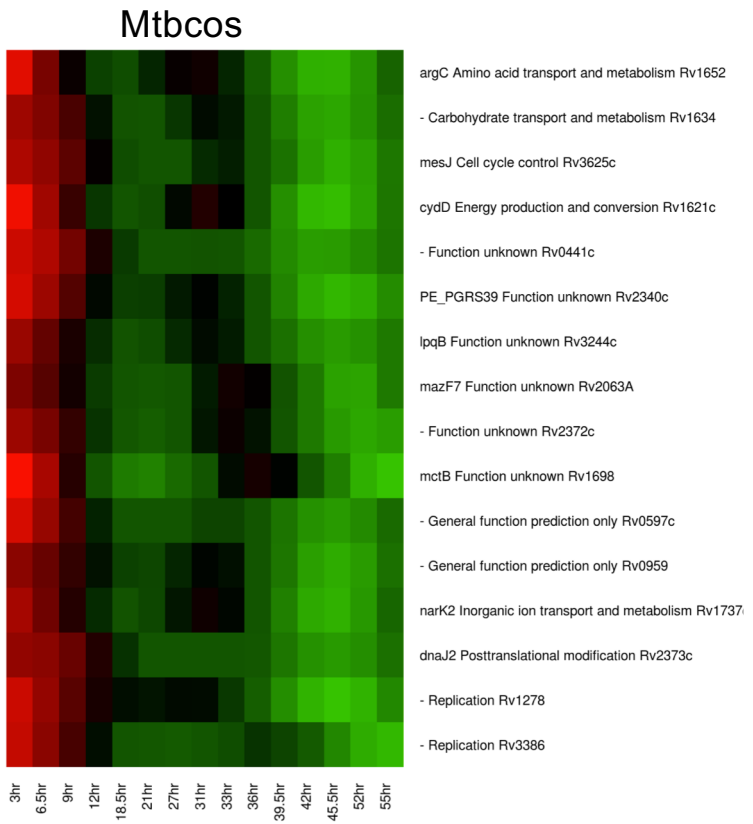
Mtbcos
argC Amino acid transport and metabolism Rv1652
- Carbohydrate transport and metabolism Rv1634
mesJ Cell cycle control Rv3625c
cydD Energy production and conversion Rv1621c
- Function unknown Rv0441c
PE_PGRS39 Function unknown Rv2340c
lpqB Function unknown Rv3244c
mazF7 Function unknown Rv2063A
- Function unknown Rv2372c
mctB Function unknown Rv1698
- General function prediction only Rv0597c
- General function prediction only Rv0959
narK2 Inorganic ion transport and metabolism Rv1737
dnaJ2 Posttranslational modification Rv2373c
- Replication Rv1278
- Replication Rv3386
3hr
6.5hr
9hr
12hr
18.5hr
21hr
27hr
31hr
33hr
36hr
39.5hr
42hr
45.5hr
52hr
55hr

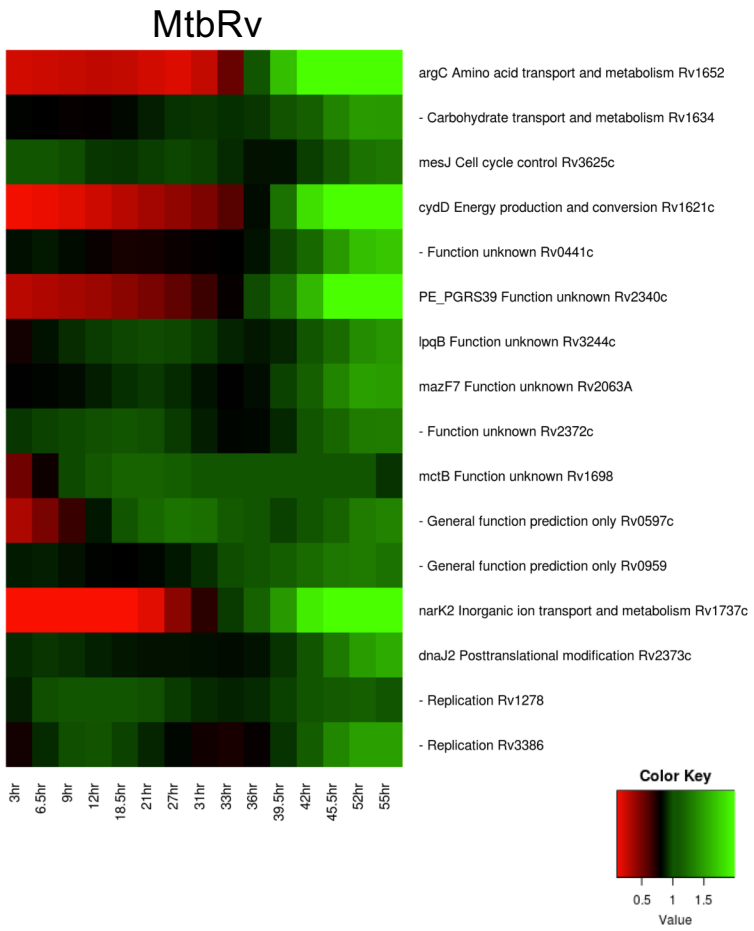
MtbRv
argC Amino acid transport and metabolism Rv1652
- Carbohydrate transport and metabolism Rv1634
mesJ Cell cycle control Rv3625c
cydD Energy production and conversion Rv1621c
- Function unknown Rv0441c
PE_PGRS39 Function unknown Rv2340c
lpqB Function unknown Rv3244c
mazF7 Function unknown Rv2063A
- Function unknown Rv2372c
mctB Function unknown Rv1698
- General function prediction only Rv0597c
- General function prediction only Rv0959
narK2 Inorganic ion transport and metabolism Rv1737c
dnaJ2 Posttranslational modification Rv2373c
- Replication Rv1278
- Replication Rv3386
3hr
6.5hr
9hr
12hr
18.5hr
21hr
27hr
31hr
33hr
36hr
39.5hr
42hr
45.5hr
52hr
55hr
Color Key
0.5
1
1.5
Value